Response to Referee 1 (Referee's comments in blue, response in black)

This paper analyses CO simulations by a chemistry climate model in order to better understand possible reasons for reported low-biases in CO, especially on the NH. To this end, a rather complicated set-up in presented in which a kind of ad-hoc inverse modeling approach is combined with ad-hoc data-assimilation. Nevertheless, some nice insight is gained in the possible causes for model-data mismatches. I have two major comments, which I outline below. I think the authors should address these issues carefully.

We thank the Referee for the constructive comments. We have incorporated these comments into our revised manuscript, as described below.

1. Major comments:
Structure of the paper.
The structure is rather messy. I think the introduction, method, and results should be better separated to improve readability. For instance, section 2.2.4 clearly presents results, but is presented in the method section. Section 3.4 presents a section thatstarts with "The primary source of OH" that I would classify as "Introduction".

We reorganized some sections of the paper to improve readability. In particular, we moved the comparison of simulated OH fields from section 2.2.4 to the Results section. We moved some of the background information on OH from section 3.4 to the Introduction.

Section3.3 suddenly ends with something about TCO, which seems more appropriate in section 3.4.1.

We discuss TCO in section 3.3 because this section discusses the impact of CO emissions on ozone. Section 3.4.1 discusses the impact of ozone on OH, so TCO is discussed again there.

The method description now centers around several "model options", which makes it hard to detect the strategy behind the paper.

We added the following paragraph to section 2.2 describing how we will alter CO emissions, OH, transport in a series of sensitivity studies, prior to our descriptions of the model options:

"We use a series of sensitivity studies to analyze the role of CO emissions, OH concentrations, and transport. Two methods are used to examine the sensitivity of CO concentrations to CO emissions from different sources: scaling up the CO emissions, and scaling up CO tracers tagged by source. We quantify the sensitivity of CO to OH concentrations by applying scaling factors to the OH field. We analyze the sensitivity to transport by comparing a free running CCM simulation with a

simulation that has prescribed meteorology. Several different chemistry options within the GEOSCCM framework are used to isolate specific processes."

Also, the forward referencing to the sensitivity simulations (page 20311: "We conduct a sensitivity simulation, described in section 3.2") makes the paper very sketchy. I would rather prefer to start with table 1 and slowly describe all the simulations in sequential order. The problem is, I guess, that the sensitivity simulations follow from the first results. I that respect, it would also be an option to follow that line and first present and discuss the reference simulations, motivate the sensitivity simulations, and then present those. Anyhow, the authors should improve the readability by severely reshuffling the paper.

We removed the forward referencing of the sensitivity studies from the Methods section. We follow the reviewer's second option of first presenting results of the reference simulations and using these results to motivate the sensitivity studies. In particular, we combined section 3.2.3 with section 3.3 and use the results of section 3.2 to motivate the sensitivity study described in section 3.3. We state, "The tagged tracer results presented in Section 3.2.2 suggest that increasing CO emissions can improve the agreement with CO surface observations. However, increasing CO emissions will lead to feedbacks on OH, CH₄, and ozone that are not captured by the COonly chemistry option. We therefore conduct a sensitivity simulation with the GMI chemistry option called GMI-HiEmis that is identical to the RefGMI simulation except for an increase in CO emissions. "

Unclear choice of presenting the results
One might question the rather ad-hoc way in which the sensitivity simulations are set up. As the authors know, there are more formal "inverse modeling" methods to optimize emissions and OH to improve the match between model and observations that are based on the minimization of a cost function. I agree that the selected ad-hoc inversion is an attractive alternative. However, what I find disturbing is the poor definition of the "cost function".

Our study is designed as a series of sensitivity studies conducted using a forward model rather than as an inverse modeling or data assimilation study. Consequently, we do not apply a cost function and instead treat the observations as "truth" to evaluate our reference and sensitivity simulations against. It is not our intention to optimize CO emissions, but rather to "investigate how attributing a CCM's CO bias to CO emissions versus OH chemistry impacts ozone and methane lifetime", as we now state in the introduction. We also added the following text in section 3.3 to clarify this: "The purpose of this experiment is not to calculate the optimum CO emissions to reproduce the CO observations, but rather to determine how a reasonable set of CO emission adjustments impacts the simulated concentrations of ozone and OH as well as CO."

The sensitivity studies described in Section 3.4 are designed to address specific hypotheses about the causes of OH asymmetry and bias. We realize that OH could

be adjusted through formal data assimilation. However, we believe that our approach of using existing reanalysis and assimilation products one at a time as inputs to our model provides an easily interpreted framework for isolating the effects of specific model biases on the CO-OH-CH$_4$ system. In this respect, our work complements the existing inversion and data assimilation studies in the literature.

Figure 3 (section 3.2.1) focuses on the latitudinal GMD CO observations between March and August, and for spring and summer individually. Why is the rest of the season left out? Figure 4 goes more quantitative, but now uses March through May (?). Figure 5 focuses on June through August, but again the rest of the year is left out from the analysis. It remains also unclear when the emission and OH changes are applied. Is this during the whole simulation (including Jan-March) or only in the months under investigation? This latter question is linked to section 3.2.3 in which emissions are changed in each season (table 3 (and not 2)).

We now explain in Section 3.2 that: "We focus on spring since it is the season with the largest bias in NH OH (Fig. 2), and contrast the spring results with those from summer, since the bias persists into summer despite seasonal differences in transport and chemistry." We now clarify that this is the focus in the introduction as well, stating "Our focus is primarily on NH spring and summer, when the NH CO bias is large.", and in section 3.2. We also clarify in section 3.2.1 that OH is reduced throughout the year. We apply the OH reduction over the whole year because the reduction is based on the methane and methyl chloroform lifetime results of Naik et al (2013), which are for the whole year. Similarly, we consider the whole year in our analyses in Section 3.4 and in Tables 2 and 4 since we are comparing methane lifetime to year-round observation-based estimates. We now state in Section 3.4: "We analyze the results for the entire year in order to compare our results to observation-based estimates of methane lifetime."

This analysis now focuses on April 2007 (why?), and shows strange results in table 3. The zero increments in Sep-Dec are intriguing, as are the exact same increments that are required for Asian / EU emissions and Russian BB. These results look rather suspect to me. It becomes even more complicated when MOPITT results are further considered (section3.2.4) when it turns out that some selected adjustments are incompatible with MOPITT (again focusing on April 2007 only).

We updated figures 6 and 7 to show the multi-year average of March-May to make the comparison to MOPITT more consistent with the time period discussed elsewhere. We did not adjust the emissions for September through December since the RefGMI simulation shows relatively little bias in Northern Hemisphere CO during these months, and our focus is on Spring and Summer.   Since our emission adjustments are based on only two constraints (the global mean bias and the interhemispheric gradient), we do not attempt to independently adjust all the different sources. Instead, we apply the same adjustment to Asia anthropogenic, European anthropogenic, and Russian biomass burning emissions. We now clarify this in section 3.3:

"We do not alter the September through December emissions since the RefGMI simulation shows little NH bias in those months (Fig. 2) and our focus is on spring and summer. We choose the adjustment factors by solving for the linear combination of COaa+COea+COrubb and COtrbb that minimizes the error in both the IHG and the global mean bias. Table 3 shows the emissions adjustments for each season. We apply the same adjustment to COaa, COea, and COrubb since these three sources show nearly the same slope (IHG bias / model bias) in Figures 4 and 5."

We also combined the Russian biomass burning line with the European and Asian anthropogenic line in Table 3 to avoid confusion.

As described above, we have clarified that our focus is on spring and summer, and that the goal is to examine the sensitivity of simulated methane lifetime and ozone to different assumptions about the cause of CO bias.

2. Minor issues:
The title does not seem to cover the contents of the paper. The paper is only partly about the methane lifetime. Maybe: "Analysis of the carbon monoxide bias in chemistry climate models".

We changed the title to "Implications of Carbon Monoxide Bias for Methane Lifetime and Atmospheric Composition in Chemistry Climate Models"

Page 20306, line 16: CO only contributes to O3 formation at sufficiently high NOx concentrations. Please add the role of NOx.

We added "where sufficient NO_x is present"

Page 20307, line 25: "consistency of CO emission estimates with surface and satellite observations": this now sounds as if emission estimates are measured at the surface and by satellites. Please make clear that there is a model in between.

We reworded this sentence to "Previous studies used models to examine the consistency of CO emission estimates with surface and satellite observations of CO concentration."

Page 20311, line 17: What are these co-emitted NMHCs? It sounds rather misty that on page 20312, line 15 these co-emitted emissions are reduced. Is this a kind of fudge factor? Are these anthropogenic NMHCs or natural? Please clarify.

Both biomass burning and anthropogenic sources that emit CO typically emit Non-Methane Hydrocarbons (NMHCs) as well, and these NMHCs eventually oxidize to from CO. Since NMHCs are not explicitly modeled in the COonly chemistry option, we account for their effect on CO through the inclusion of a CO amplification factor. A detailed description of this process is provided in Duncan et al. (2007a), which we cite here and discuss in the introduction. The choice of CO amplification factor is chemical mechanism-dependent, since it is intended to account for processes that are left out of the chemical mechanism, which is why it differs between the CO-OH and COonly chemistry options. We now clarify that these are from both anthropogenic and biomass burning sources.

Page 20313, line 25: "during" NH spring.

Done.

Page 20316, line 28: table 3.

Done

Page 20317, line 1: and b shows → and b show

Done

Page 20318, section 3.2.5: I find these results interesting. Has a reason been identified for the different transport? Which transport patterns have been identified as the best? Presumably vertical transport differs in MERRA, and this is an assimilation product, which is consistent with observations, hence better? Could this important observation be mentioned more clearly, e.g. in the abstract?

We now mention in the abstract that the use of specified meteorology improves the comparison with surface observations: "We find that the use of specified meteorology alters the distribution of CO compared to a free-running CCM simulation, improving the comparison with surface observations in summer". We expect the horizontal winds to be better in MERRA, which will influence tracer distributions. Vertical transport is not constrained by observations in MERRA, so it is not clear which is best in that regard. This is an interesting subject for future work, but is beyond the scope of the current study.

Page 20320, line 22: The increased OH → The decreased OH Page 20323, line 11 (and section 3.4.4 in general): Are there observational indications (e.g. from satellite data) that NOx emissions are too high (a known bias)? Also, reducing the NOx concentrations by 30% will affect not only the OH recycling (HO2 + NO), but also the O3 production. Do I understand correctly that these effects are ignored here, because O3 columns are also prescribed in the RefCO-OH simulations? Please mention this clearly. Do you proportionally adjust NO and NO2?

This sensitivity study is not based on observational evidence of NO_x bias, but rather on the known sensitivity of OH to NO_x concentrations and the hemispheric asymmetry in NO_x emissions. The reviewer is correct that the impact of changing NO_x on O_3 production is ignored here, since the O_3 field is prescribed. We now mention this in Section 3.4.4: "We note that in this experiment, ozone values remain the same as in RefCO-OH, rather than responding to the change in NO_x.". We also clarified that NO and NO_2 are both reduced by 30%.

Page 20325, line 14: Linked to the above: "reducing the uncertainties in NOx emissions": this would call for a similar approach using e.g. NO2 column observations from OMI/GOMe-2, like Miyasaki, 2012.

We added the following sentence in Section 3.4.4: "Previous studies have estimated NO_x emissions based on satellite observations of NO_2 columns (Lamsal et al., 2011; Miyazaki et al., 2012a), but some uncertainty in NO_x emissions remains."

Response to Referee 2 (Referee's comments in blue, response in black)

It is a well-know problem that current chemistry models are unable to represent the magnitude of carbon monoxide (CO) in the northern hemisphere, particularly in winter and spring. This paper addresses this problem and highlights the sensitivity of modeled CO to emissions and hydroxyl radical (OH) concentrations. They then go on to provide a valuable insight into the importance of model biases in ozone, water vapor and nitrogen oxide emissions in driving possible biases in simulated OH concentrations. The paper is well presented and scientifically relevant and is well suited for publication in ACP after the relatively minor corrections that are listed below.

We thank the Referee for the positive review. We incorporated the specific comments as described below.

Main comments:

One of my main questions is why you use a chemistry climate model with free-running meteorology instead of a model with specified dynamics as your primary model. You show that when you use specified dynamics in the CO-only runs you reduce the model bias so I wonder what results you would get in section 3.4 if you also try a run with SD? It would be useful to give a brief description of why you employed each model version under section 2.2, as you have done for the CO-OH option on page 20312, L17.

Our goal is to understand the CO bias in free-running CCMs, since they are used to predict past and future changes in methane lifetime and other trace gas concentrations. We added the following explanation of this choice in Section 3.2.4: "The simulations discussed so far are free-running CCM simulations driven by SSTs, since our goal is to understand the biases seen in CCM studies such as ACCMIP." Following the reviewer's suggestion, we also added an explanation of what we use each chemistry option for to the explanation of the GMI chemistry and CO-only chemistry options in section 2.2, to match what we did for the CO-OH option: "We use the GMI chemistry option to quantify the impact of changes in CO emissions on methane, OH, and ozone." and "We use the CO-only option to calculate the influence of specific sources on CO concentrations, and to isolate the impact of specific changes in OH on CO."

Under section 2 give a brief description of how you change emissions, transport and OH prior to describing results. (Just simply by saying you apply scaling factors to emissions/OH and by switching between free-running and SD meteorology).

We added a paragraph describing this to section 2.2:

"We use a series of sensitivity studies to analyze the role of CO emissions, OH concentrations, and transport. Two methods are used to examine the sensitivity of

CO concentrations to CO emissions from different sources: scaling up the CO emissions, and scaling up CO tracers tagged by source. We quantify the sensitivity of CO to OH concentrations by applying scaling factors to the OH field. We analyze the sensitivity to transport by comparing a free running CCM simulation with a simulation that has prescribed meteorology. Several different chemistry options within the GEOSCCM framework are used to isolate specific processes."

Table 2: Add CO-only option for the OH information. It is useful to see what the OH looks like in the CO-only run and whether it differs from the CO-OH model. Consider also adding zonal mean plot of OH for CO-only simulation to figure 1.

The CO-only run uses the OH field generated by the RefGMI simulation. We do not show it in the table or figure because it would be identical to the RefGMI OH, which is already shown. We modified the wording in section 2.2.2 to clarify that the OH in the RefCOonly simulation is from the RefGMI simulation, replacing "ACCMIP" with "RefGMI".

Figure 3: Can you show bias instead of absolute concentrations – may be easier to see differences between the runs?

We prefer to show the absolute concentrations so that we can also show the observations.

Pg20314 L9-11 – How different are the NOx, NMHC and CH4 archived fields used for the CO-OH runs compared to those calculated within the RefGMI run? Does this explain the OH differences or is it something else?

The archived NO_x, NMHC, and CH_4 archived fields are taken from the RefGMI run, so this does not explain the OH differences. We clarified that these are fields are from the RefGMI run in section 2.2.3 by replacing "ACCMIP" with "RefGMI".

Pg 20316, L8: Why exclude COnaa and CObio? Move this sentence to L13, after you've highlighted problems in increasing these regional emissions.

Done

Pg 20319, Section 3.3: How do you sample the model for comparison to the MLS/OMI total column ozone. Does the instrument see the full total atmospheric column of ozone? Do you remove any model data when there is missing observations? Are there any limitations that will have an impact on your results?

We now mention in section 3.4.1 that "No scaling is applied where the TCO data is missing". We added to Section 2.1: "The observations are cloud-filtered, so there is sensitivity throughout the troposphere, although there is some reduction in retrieval efficiency in the lower troposphere. "

We reworded this sentence and added citations: "Carbon monoxide (CO) is an ozone precursor and a major sink of the hydroxyl radical (OH) in the troposphere [Logan et al., 1981; Spivakovsky et al., 2000]."

Yes, except for Trinidad Head, which is averaged over 2002-2009, since earlier data was not available. We added the year information to the text, stating "Observations are averaged over the period from 1999 to 2009, with the exception of Trinidad Head, which is averaged over 2002-2009."

Done

Global mean bias. We corrected this text to say "in the global mean".

Done

Done

Done

Implications of Carbon Monoxide Bias for Methane Lifetime and Atmospheric Composition in Chemistry Climate Models

S. A. Strode[1,2], B. N. Duncan[2], E. A. Yegorova[2,3,*], J. Kouatchou[2,4], J. R. Ziemke[2,5], A. R. Douglass[2]

[1]Universities Space Research Association, Columbia, MD, USA

[2]NASA Goddard Space Flight Center, Greenbelt, MD, USA

[3]Earth System Science Interdisciplinary Center, College Park, MD, USA

[4]Science Systems and Applications Inc., Lanham, MD, USA

[5]Morgan State University, Baltimore, MD, USA

* Now at Nuclear Regulatory Commission, Rockville, MD, USA

Correspondence to: Sarah Strode Sarah.a.strode@nasa.gov

Abstract

A low bias in carbon monoxide (CO) at northern high and mid-latitudes is a common feature of chemistry climate models (CCMs) that may indicate or contribute to a high bias in simulated OH and corresponding low bias in methane lifetime. We use simulations with CO tagged by source type to investigate the sensitivity of the CO bias to CO emissions, transport, global mean OH, and the hemispheric asymmetry of OH. We also investigate how each of these possible contributors to the CO bias affects the methane lifetime. We find that the use of specified meteorology alters the distribution of

1

CO compared to a free-running CCM simulation, improving the comparison with surface observations in summer. Our results also show that reducing the hemispheric asymmetry of OH improves the agreement of simulated CO with observations. We use simulations with parameterized OH to quantify the impact of known model biases on simulated OH. Removing biases in ozone and water vapor as well as reducing northern hemisphere NO_x does not remove the hemispheric asymmetry in OH, but reduces global mean OH by 18%, bringing the simulated methane lifetime into agreement with observation-based estimates.

1   Introduction

Carbon monoxide (CO) is an ozone precursor and a major sink of the hydroxyl radical (OH) in the troposphere [Logan et al., 1981; Spivakovsky et al., 2000]. Consequently, CO indirectly impacts climate by increasing tropospheric ozone where sufficient NO_x is present and increasing the lifetimes of methane and other short-lived greenhouse gases (GHGs), as well as eventually oxidizing to CO_2 (e.g. Prather, 1996; IPCC, 1990). The effect of CO on OH also leads to impacts on oxidation of SO_2 to sulfate, providing another climate forcing (Shindell et al., 2009). Previous studies calculated global warming potentials due to these effects using box models (Daniel and Solomon, 1998), 2-dimensional models (Fuglestvedt et al., 1996; Johnson and Derwent, 1996), or 3-dimensional models (Derwent et al., 2001; Fry et al., 2013; Berntsen et al., 2005; Shindell et al., 2009; Fry et al., 2012). Since neither CO nor ozone is well mixed in the atmosphere, the location of the CO perturbation affects its climate impact. CO emissions in the tropics have a greater impact on ozone radiative forcing than emissions at high latitudes (Bowman and Henze, 2012) due the intense photochemistry in the

2

tropics as well as the presence of deep convection, which can loft ozone precursors to the upper troposphere where the ozone radiative forcing is greatest (Fry et al., 2013; Naik et al., 2005).

While a large number of modeling studies have investigated the sources, transport, and distribution of CO, global models often show major biases compared to observations. A study of 26 atmospheric chemistry models found that the simulated CO was biased low in the extratropical northern hemisphere (Shindell et al., 2006) compared to satellite observations from MOPITT (Emmons et al., 2004) and surface observations, especially during spring. Shindell et al. (2006) attribute this bias primarily to an underestimate in northern hemisphere (NH) CO emissions, particularly from Asia. Monks et al. (2015) found that arctic CO is biased low in the multi-model POLARCAT Model Intercomparison Project (POLMIP), and identified differences in global OH concentrations as a major driver of the inter-model differences in arctic CO. The multi-model mean of the Atmospheric Chemistry and Climate Model Intercomparison Project (ACCMIP) simulations also shows a negative bias compared to both MOPITT and surface observations in the northern extratropics (Naik et al., 2013). Naik et al. (2013) found that ACCMIP models underestimate the methane and methyl chloroform lifetimes compared to the observation-based estimates of Prinn et al. (2005) and Prather et al. (2012) and produce a high bias in the NH to southern hemisphere (SH) ratio of OH, consistent with the underestimate of NH CO. A recent comparison of simulated and observed methyl chloroform levels also indicates that the NH/SH OH ratio is 0.97 ± 0.12 rather than the value of 1.28 calculated by the ACCMIP models (Patra et al., 2014).

3

However, OH and CO are major losses for each other, complicating the determination of how much CO bias drives OH bias versus OH bias driving CO bias.

Previous studies used models to examine the consistency of CO emission estimates with surface and satellite observations of CO concentration. A modeling study by Duncan et al. (2007a) showed that their model compared well to observations in the NH extratropics, but they point out that a low bias in their model emissions may have been compensated by an assumption made in their simplified chemical scheme that non-methane hydrocarbons (NMHCs) oxidize to CO immediately upon release; this assumption is valid during summer months for short-lived NMHCs (e.g., alkenes, isoprene), but is not valid in winter and spring for longer-lived NMHCS (e.g., alkanes). Stein et al. (2014) found that a combination of higher winter traffic emissions from North America and Europe and reduced dry deposition during boreal winter improved the agreement between simulated and observed CO. These findings are consistent with inversions of MOPITT CO data that show that including greater winter emissions from the NH reduces the negative bias in springtime CO at northern latitudes (Petron et al., 2004).

Kopacz et al. (2010) inverted CO observations from multiple satellites and concluded that northern mid-latitude CO sources were underestimated in winter, and that implementing large seasonal variations in emissions improved model agreement with observations. The inversion study of Fortems-Cheiney et al. (2011) also found that the posterior CO emissions had large seasonality in the NH, with the maximum occurring in spring. However, the source strengths estimated by inversions are influenced by factors such as model transport (Arellano and Hess, 2006) and the concentrations of other

4

Deleted: modeling

Deleted: d

Deleted: Their

Deleted: is

species that interact with CO through OH chemistry (Pison et al., 2009; Muller and Stavrakou, 2005; Jones et al., 2009). Given the complexities of the nonlinear CO-OH-CH_4 system, we conduct a series of sensitivity studies in which we adjust individual inputs to a chemistry climate model (CCM) one at a time.

Uncertainty in the tropospheric burden and distribution of OH leads to further uncertainty in the CO budget. Hooghiemstra et al. (2011) found that higher NH OH concentrations led to higher anthropogenic CO emissions in their inversion study, while lower OH concentrations over tropical land masses and the SH led to lower biomass burning CO emissions and less CO from NMHCs. Duncan et al. (2007a) found that reducing OH by 20% globally improved the comparison of their simulated CO with surface observations in some locations, but degraded the comparison at other locations. Patra et al. (2014) suggested that top-down emission estimates from models with much higher OH in the NH than SH likely overestimate NH countries' emissions of CO and other reactive species. Mao et al. (2013) found that including conversion of HO_2 to H_2O on aerosols reduced OH concentrations in a global model, correcting much of the negative model bias in the extratropical NH with the largest CO increase occurring in spring.

Accurate simulation of tropospheric OH requires models to represent multiple drivers of atmospheric OH concentrations. Holmes et al. (2013) found that temperature, water vapor, stratospheric ozone, and emissions from biomass burning and lightning could together explain most of the interannual variability in methane lifetime against OH. Duncan and Logan (2008) found that changes in the ozone column were a major driver of OH variability over 1988-1997. Murray et al. (2013) found that lightning was more

5

important for OH variability over 1998-2006, when there was less variability in the overhead ozone column.   Murray et al. (2014) found that on glacial-interglacial timescales, OH concentrations were proportional to the tropospheric ozone photolysis rate, specific humidity, and reactive nitrogen emissions, and inversely proportional to CO emissions.   The present study investigates the sensitivity of simulated CO and methane lifetime to biases in some of these processes.

Understanding the causes and implications of CO bias in CCMs is important for climate prediction as it may indicate or contribute to biases in methane and ozone and their respective radiative forcing contributions. The goal of this study is to quantify the relationship of the extratropical NH CO bias seen in CCMs with bias in oxidant concentrations and methane lifetime. Our focus is primarily on NH spring and summer, when the NH CO bias is large.   We use the GEOS-5 Chemistry Climate Model (GEOSCCM) to investigate how attributing a CCM's CO bias to CO emissions versus OH chemistry impacts ozone and methane lifetime. We also quantify the contribution of model biases in other constituents such as ozone and water vapor to the simulated OH and CO distributions and methane lifetime.

2   Methods

2.1   Constituent Observations and Assimilated Fields

Our primary constraint on the model CO distribution comes from surface observations from the NOAA Global Modeling Division (GMD) network (Novelli and Masarie, 2014). We use the monthly mean data. The MOPITT instrument on the TERRA satellite provides additional constraints on the CO distribution. MOPITT provides almost

6

global coverage every three days from March 2000 to present (Edwards et al., 2004). We use the level 3 CO column data from the MOPITT version 5 thermal infrared (TIR) product (Deeter et al., 2011; Deeter et al., 2013).

Observations of tropospheric ozone are important for constraining the source of OH. Ziemke et al. (2011) created a climatology of tropospheric column ozone (TCO) based on the difference between the stratospheric column ozone (SCO) from the Microwave Limb Sounder (MLS) and total ozone column data from the Ozone Monitoring Instrument (OMI). The observations are cloud-filtered, so there is sensitivity throughout the troposphere, although there is some reduction in retrieval efficiency in the lower troposphere. We use the TCO product for 2004-2010 to constrain the tropospheric ozone column. Stratospheric ozone is also important for constraining the OH source due to its effect on photolysis (Rohrer and Berresheim, 2006). We use the Global Modeling and Assimilation Office (GMAO) ozone assimilation product for 2005-2010 to constrain stratospheric ozone concentrations. The GMAO assimilated ozone product, described in (Ziemke et al., 2014; Wargan et al., 2015), is a gridded product that was created by ingesting MLS ozone profiles and OMI total column ozone into the GEOS-5 assimilation system.

Water vapor is another important influence on OH concentrations. We use specific humidity from the Modern-Era Retrospective Analysis for Research and Applications (MERRA) (Rienecker et al., 2011).

2.2 Model and Methodology

Our analysis uses the GEOSCCM to assess possible causes and impacts of CO and OH bias. After spin-up, we conduct a series of time slice simulations of 1999-2009 with

7

fixed emissions using observed sea surface temperatures (SSTs) to drive the CCM meteorology, and then average our results over all years of the time slice. All simulations use the Fortuna version of GEOS-5 (Molod et al., 2012) and have 2 degree latitude by 2.5 degree longitude horizontal resolution and 72 vertical levels.

We use a series of sensitivity studies to analyze the role of CO emissions, OH concentrations, and transport. Two methods are used to examine the sensitivity of CO concentrations to CO emissions from different sources: scaling up the CO emissions, and scaling up CO tracers tagged by source. We quantify the sensitivity of CO to OH concentrations by applying scaling factors to the OH field. We analyze the sensitivity to transport by comparing a free running CCM simulation with a simulation that has prescribed meteorology. Several different chemistry options within the GEOSCCM framework are used to isolate specific processes. We describe each chemistry option and associated experiments below and in Table 1.

2.2.1 GMI Chemistry option

GEOSCCM integrates the chemistry mechanism of the Global Modeling Initiative (GMI) CTM (Duncan et al., 2007b; Strahan et al., 2007) into the GEOS-5 Atmospheric GCM (AGCM). The GMI chemistry includes a comprehensive mechanism of tropospheric and stratospheric chemistry, including 117 species and over 400 reactions. The reference simulation for this study, hereafter called RefGMI, is the year 2000 timeslice simulation conducted for the ACCMIP intercomparison. The configuration of the ACCMIP simulations is described in Lamarque et al. (2013). The biases in CO and methane lifetime seen in the GEOSCCM simulation are similar to those seen in the ACCMIP multi-model mean (Naik et al., 2013). Consequently, our analyses of bias in

the GEOSCCM are likely applicable to other CCMs as well. We use the GMI chemistry option to quantify the impact of changes in CO emissions on methane, OH, and ozone.

2.2.2 CO-only Option

GEOSCCM includes a CO-only option to "tag" CO according to source type or location (Bian et al., 2010). This simplified chemistry option allows us to separate the contributions of different CO sources and to quantify the impact of a specific change in OH. In this chemistry option, the loss of CO is calculated based on prescribed OH fields, so changes in CO do not feed back onto OH. Our reference tagged-CO simulation, called RefCOonly, uses monthly OH fields archived from the RefGMI simulation, and the CO sources from methane and isoprene oxidation are calculated using monthly methane and isoprene fields archived from RefGMI as well. Emissions and other forcings are chosen to parallel the RefGMI simulation; however, the COonly option includes an amplification factor for anthropogenic and biomass burning CO emissions to account for the absence of co-emitted NMHCs (Duncan et al., 2007a). We use the CO-only option to calculate the influence of specific sources on CO concentrations, and to isolate the impact of specific changes in OH on CO.

The GEOSCCM includes an option to constrain the meteorology with MERRA or any GMAO assimilation product. The simulation is pulled towards the MERRA analysis through application of an incremental analysis update (Bloom et al., 1996), calculated every six hours from comparison of the simulation with the analysis. We conduct a COonly simulation with specified dynamics from MERRA, which we refer to as COonlySD, where "SD" stands for "specified dynamics". The COonlySD simulation has

9

the same emissions and OH field as RefCOonly, but the tracer transport will differ between the two simulations.

2.2.3 CO-OH Option

A third chemistry option within the GEOSCCM is the CO-OH option (Duncan et al., 2000; Duncan et al., 2007a). This chemistry option is of intermediate complexity between the GMI and Tagged-CO options. This option is similar to the CO-only option except that OH is calculated interactively, providing a feedback between CO and OH concentrations. In our reference simulation with this option, RefCO-OH, chemistry inputs to the parameterization of OH such as ozone, NO_x, CH_4, and NMHC concentrations are prescribed from the archived monthly output of the RefGMI simulation. The temperature, water vapor, and irradiance-related variables input to the parameterization are calculated within the CCM. Since the parameterization was only designed to provide tropospheric OH values, we use the results of the parameterization from the surface to 300 hPa, and archived OH fields taken from the RefGMI simulation above 300 hPa. The CO emission amplification factors are adjusted slightly downward compared to the CO-only simulation to bring the RefCO-OH simulation into better agreement with the RefGMI simulation. We use the CO-OH option to examine how biases in a particular model field such as ozone affect OH and CO concentrations.

3   Results

We use the three chemistry options of the GEOSCCM to separate the contributions of emissions, chemistry, and transport to model bias in CO and methane lifetime. In Section

10

Deleted: parameterization

Deleted: of

Deleted: , and was designed to represent an older version of the chemistry scheme used in the GMI chemistry option

Deleted: parameterization

Deleted: ACCMIP

Deleted: GMI-chemistry

Deleted: .

Deleted: Section 3.4 describes sensitivity studies conducted with this option.

Deleted: <#>Comparison of OH between Chemistry Options .

Moved down [1]: The choice of chemistry option affects the CO and OH distributions produced by the GEOSCCM. Annually averaged OH is higher in the RefGMI simulation in both hemispheres (Table 2; Fig. 1). High OH values extend further down in the troposphere in RefGMI than in RefCO-OH. Global annual mean mass-weighted tropospheric OH is approximately 7% lower in RefCO-OH than in RefGMI, but the NH/SH OH ratio is marginally higher: 1.22 instead of 1.19. *Prather et al.* [2012] report an observation-based estimate of methane lifetime of 9.1±0.9 years, and a methane lifetime against tropospheric OH of 11.2±1.3 years. The lifetimes of methyl chloroform and methane against tropospheric OH in the RefGMI simulation are 5.9 and 9.6 years, respectively (Table 2). The lifetimes of methyl chloroform and methane against tropospheric OH in the RefCO-OH simulation are 6.4 years and 10 years, respectively, within the uncertainty of the observation-based estimates. The seasonal cycles are similar in both simulations, but the difference in NH OH is larger in the first half of the year than the second half (Fig. 1d). Consequently, when using the CO-OH parameterization to investigate OH and CO, we present the changes due to a given factor rather than the absolute values of CO, OH, and methane lifetime for easier comparison with the other simulations. .

3.1, we compare the CO distribution simulated by the three options to observations and discuss the consistencies and differences between simulations. We analyze the impacts of increasing emissions, decreasing OH, and changing model transport on the CO distribution in Section 3.2, and examine how changing CO emissions affects ozone and OH in Section 3.3. In Section 3.4, we investigate the contribution of known model biases to simulated OH and methane lifetimes. Table 1 summarizes the key results of each of the sensitivity studies.

3.1 Comparison of OH and CO in the Reference Simulations and Observations

This section presents a comparison of CO and OH distributions from the RefGMI, RefCO-only, and RefCO-OH simulations to each other and to observations. The choice of chemistry option affects the CO and OH distributions produced by the GEOSCCM. Annually averaged OH is higher in the RefGMI simulation in both hemispheres (Table 2; Fig. 1). High OH values extend further down in the troposphere in RefGMI than in RefCO-OH. Global annual mean mass-weighted tropospheric OH is approximately 7% lower in RefCO-OH than in RefGMI, but the NH/SH OH ratio is marginally higher: 1.22 instead of 1.19. *Prather et al.* [2012] report an observation-based estimate of methane lifetime of 9.1+0.9 years, and a methane lifetime against tropospheric OH of 11.2+1.3 years. The lifetimes of methyl chloroform and methane against tropospheric OH in the RefGMI simulation are 5.9 and 9.6 years, respectively (Table 2). The lifetimes of methyl chloroform and methane against tropospheric OH in the RefCO-OH simulation are 6.4 years and 10 years, respectively, within the uncertainty of the observation-based estimates. The seasonal cycles are similar in both simulations, but the difference in NH

11

OH is larger in the first half of the year than the second half (Fig. 1d). Consequently, when using the CO-OH option, we present the changes due to a given factor rather than the absolute values of CO, OH, and methane lifetime for easier comparison with the other simulations.

Figure 2 shows the annual cycle of simulated CO and observations from six GMD sites selected to represent a range of latitudes. Observations are averaged over the period from 1999 to 2009, with the exception of Trinidad Head, which is averaged over 2002-2009. The RefGMI simulation (purple) is biased low at the NH sites, with the bias most prominent during the first half of the year, especially NH spring. The simulation shows less bias at the SH sites, but some negative bias is evident in SH spring. The RefCOonly simulation (green) shows similar results to RefGMI, including a large negative bias in the NH in spring. Consequently, diagnosing the cause of bias in the RefCOonly simulation can provide insight into the bias in the RefGMI simulation.

The RefCO-OH simulation (orange) shows less springtime bias compared to observations than the RefGMI and RefCOonly simulations. However, its annual cycle is shifted later, resulting in more negative biases in September-December at the higher northern latitudes. The difference between the RefCO-OH and the other two reference simulations is explained by the differences in the OH field calculated by the parameterization compared to that calculated by the GMI chemistry mechanism. In April, when the greater NH bias of the RefGMI simulation is most evident (Fig. 2), the RefGMI OH is markedly higher than the RefCO-OH OH (Fig. 1).

12

Deleted: parameteriza

Deleted: to investigate OH and CO

Deleted: compares

Deleted: in simulations to

Deleted: in

3.2   Sensitivity of simulated CO to sources, OH, and transport

We conduct a series of sensitivity studies to examine possible causes of the bias in NH CO seen in the Ref-GMI and Ref-COonly simulations during spring and summer. We focus on spring since it is the season with the largest bias in NH OH (Fig. 2), and contrast the spring results with those from summer, since the bias persists into summer despite seasonal differences in transport and chemistry.

3.2.1   Sensitivity of CO-only simulations to sources and OH

Adjusting the strength of mid-latitude CO sources can reduce the bias in the interhemispheric CO gradient. We use CO-only simulations to examine the impact of increasing specific sources of CO. Following the method of Strode and Pawson (2013), we estimate the impact of increasing a particular source by increasing the tagged-CO tracer for that source and then re-computing total CO. We impose increases of 10%, 20%, 50%, 100%, and 150% for each tagged tracer. Figure 3 shows how the increased Asian anthropogenic CO (COaa) or tropical biomass burning CO (COtrbb) alters the comparison between modeled CO and the GMD CO observations as a function of latitude taken as an average of March to August. Similar results are present for spring and summer individually. An increase in COaa of approximately 100% removes the negative bias at high latitude sites, but has little effect on the small negative bias at low latitudes (Fig. 3a). CO transported southward from Asia encounters higher OH than that transported northward, leading to a shorter lifetime (Duncan and Logan, 2008). Increasing COtrbb improves the model agreement with observations at low latitudes, but creates overestimates at some tropical sites while providing only a modest reduction in the high latitude bias (Fig. 3b).

13

We examine the impact of reducing OH concentrations globally or only in the NH in our COonly simulation and find that a large decrease in NH OH is effective in reducing the high latitude CO bias. Naik et al. (2013) found that the ACCMIP multi-model mean underestimated annual mean tropospheric OH by 5-10% globally. The NH/SH OH ratios in the ACCMIP multi-model mean and GEOSCCM ACCMIP simulation are 1.28 and 1.18, respectively (Naik et al., 2013), compared to the (Patra et al., 2014) estimate of 0.97 ± 0.12. Fig 3c shows that reducing OH throughout the year by 5-10% leads to a small increase in CO across all latitudes, yielding a small reduction in the bias compared to GMD observations. Decreasing OH by 20% in the NH only leads to a large improvement in high latitude CO compared to observations, with only a small effect in the southern hemisphere.

3.2.2 Impact of sources and OH on global mean and inter-hemispheric gradient bias in CO

We find that achieving zero bias in both the inter-hemispheric gradient (IHG) and the global mean would require changes in multiple emission sources. Figure 4 illustrates how changing the concentrations of several tagged CO tracers, as well as OH, impacts the global mean bias, IHG bias, and correlation (r^2) of the simulated CO compared to the GMD observations for March through May. Increasing anthropogenic CO from Asia (COaa), Europe (COea), or North America (COnaa), or increasing Russian biomass burning (COrubb) reduces the bias in the IHG as well as in the global mean. Increasing CO from tropical biomass burning (COtrbb) leads to a smaller reduction in the IHG bias, while increasing CO from biogenic emissions (CObio) reduces the mean bias with little

Deleted: IHG

Deleted: inter-hemispheric gradient (

Deleted:)

14

effect on the IHG (Fig. 4a). Consequently, increases in both groups of emissions are necessary to simultaneously remove the global mean bias and correct the IHG.

A similar analysis for June through August (Fig. 5) shows that increasing COaa, COea, COnaa, or COrubb can eliminate the majority of the bias in both the global mean and the IHG in summer. Increasing COrubb is more effective in summer than spring since boreal biomass burning emissions are larger in summer. In contrast to the spring results, increasing COtrbb in summer leads to greater bias in the IHG. This difference occurs because tropical biomass burning occurs primarily north of the equator in March and April but shifts to the southern hemisphere in June, July, and August.

While increases in COaa, COea, COnaa, and COrubb show similar slopes for IHG versus global mean bias, increasing COnaa reduces the correlation with observations, where as increasing the other sources yields a slight improvement in correlation (Fig. 4b, 5b). Increases in both COtrbb and CObio reduce the correlation with observations in summer, but the effect is also present for CObio in spring. We therefore exclude increases in COnaa and CObio in the rest of our study.

Figures 4 and 5 also show the impact of changing OH. The sensitivity of CO to changes in OH is location dependent, with higher sensitivity in regions without strong local CO sources (Holloway et al., 2000). Reducing OH globally reduces both the IHG and global mean bias. However, reducing OH by 20% in the NH only yields a greater reduction in both biases as well as the greatest improvement in correlation. We refer to the simulation with the 20% decrease in NH OH as COonlyLowNHOH.

Moved down [3]: We exclude increases in COnaa and CObio in the rest of our study.

Moved (insertion) [3]

15

3.2.3 Impact of adjusting sources versus NH OH on comparison to observations

We next compare the impact of increasing emissions with that of reducing NH OH by 20%. We compare the COonlyLowNHOH scenario with a simulation called GMI-HiEmis that includes increased CO emissions, further described in Section 3.3. The RefCOonly simulation shows a similar surface CO distribution to RefGMI (Fig. 6a,c). The COonlyLowNHOH scenario (Fig. 6d) improves the agreement with the remote high latitude sites compared to the RefCOonly simulation, but like the HiEmis case (Fig. 6b), it leads to an overestimate of CO concentrations over Europe and eastern United States. Consequently, a combination such as reduced NH OH and reduced emissions over the eastern U.S. is likely needed to reconcile the simulated CO with observations.

Sparse surface data makes it difficult to determine from comparison with GMD observations whether the higher CO seen in GMI-HiEmis and COonlyLowNHOH is realistic (Fig. 6), so we also compare the four simulations shown in Figure 6 to the CO column from MOPITT. Both the RefGMI and RefCOonly simulations show a large negative bias in NH CO compared to MOPITT (Fig. 7a,c). The GMI-HiEmis and COonlyLowNHOH simulations both reduce this negative bias (Fig. 7b,d), but the increased emissions of the GMI-HiEmis simulation lead to a greater overestimate of CO over East Asia and Indonesia. Furthermore, eliminating the increase in COea to reduce the high bias compared to surface observations over Europe and compensating with a larger adjustment in Asian CO would lead to an even greater bias over Asia compared to MOPITT.

16

Impact of increased source strength in a GMI chemistry simulation

Based on the tagged tracer results (Figs. 4 and 5), we conduct a new simulation, called HiEmis, using the GMI chemistry with increased emissions from Asian and European anthropogenic sources as well as tropical and Russian biomass burning. All other aspects of the simulation are identical to the standard simulation. We adjust the emissions for each season based on the biases and tagged tracer sensitivities for the season. We choose the adjustment factors by solving for the linear combination of COaa+COea+COrubb and COtrbb that minimizes the error in both the IHG and the global mean bias. Table 2 shows the emissions adjustments for each season. Figure 6a,b shows the simulated surface CO for April 2007 in the RefGMI and GMI-HiEmis simulations compared to GMD observations. The HiEmis simulation shows less negative bias at many of the high latitude sites, but shows a positive bias over Europe, one of the locations where the emissions were increased. This suggests that our adjustment of COea is too large, which is unsurprising given that European emissions are relatively well known.

| Russian BB | 17.4 | 45.0 | 63.2 | 0.00 |

3.2.4 CO sensitivity to transport

Transport, in addition to chemistry and emissions, plays a role in the IHG of CO. The simulations discussed so far are free-running CCM simulations driven by SSTs, since our goal is to understand the biases seen in CCM studies such as ACCMIP. Consequently, the simulated tracer transport is affected by any differences between the simulated and actual meteorology. We examine the sensitivity of the CO bias to model transport by comparing RefCOonly, which is a free-running CCM simulation, with the COonlySD simulation, which has year-specific meteorology from MERRA.   The largest difference between the simulations occurs poleward of 30°N during July through October (Fig. 8a). The use of specified meteorology makes only a small difference in the global mean and IHG CO biases compared to surface observations in March-May (Fig. 4), but leads to a large reduction in bias as well as improved spatial correlation with the GMD observations in June-August (Fig. 5).   The biases in global mean CO and the CO IHG are -3.5% and -6.6%, respectively, in COonlySD, compared to -11% and -26%, respectively, in RefCOonly.   More CO from northern hemisphere anthropogenic and boreal biomass burning sources remains in the lower troposphere and reaches the high latitudes in COonlySD, where as more is transported to the upper troposphere in RefCOonly (Fig. 8b).

3.3 Impact of Increased CO Emissions on Ozone, OH, and CH$_4$ Lifetime

The tagged tracer results presented in Section 3.2.2 suggest that increasing CO emissions can improve the agreement with CO surface observations.   However, increasing CO emissions will lead to feedbacks on OH, CH$_4$, and ozone that are not captured by the COonly chemistry option. We therefore conduct a sensitivity simulation

17

with the GMI chemistry option called GMI-HiEmis that is identical to the RefGMI simulation except for an increase in CO emissions. Since trace gases in the GMI option of the GEOSCCM are radiatively coupled to the underlying GCM, altering emissions within this option produces feedbacks between CO, ozone, CH_4, and radiation and transport.

The results shown in figures 4 and 5 suggest that increasing CO from tropical biomass burning along with Asian anthropogenic, European anthropogenic, and Russian biomass burning CO, can eliminate both the IHG and global mean bias. We therefore adjust the emissions for winter, spring, and summer in the GMI-HiEmis simulation based on the biases and tagged tracer sensitivities for the season. We do not alter the September through December emissions since the RefGMI simulation shows little NH bias in those months (Fig. 2) and our focus is on spring and summer. We choose the adjustment factors by solving for the linear combination of COaa+COea+COrubb and COtrbb that minimizes the error in both the IHG and the global mean bias. Table 3 shows the emissions adjustments for each season. We apply the same adjustment to COaa, COea, and COrubb since these three sources show nearly the same slope (IHG bias / model bias) in Figures 4 and 5. The purpose of this experiment is not to calculate the optimum CO emissions to reproduce the CO observations, but rather to determine how a reasonable set of CO emission adjustments impacts the simulated concentrations of ozone and OH as well as CO.

Including larger CO emissions increases the loss of OH, reducing OH concentrations. The mass-weighted global mean tropospheric OH in the GMI-HiEmis simulation is 1.11×10^6 molec/cm^3, a 3% decrease compared to the RefGMI simulation (Table 2). The

18

methane lifetime against tropospheric OH also increases slightly, from 9.6 years in the RefGMI simulation to 9.9 years in the HiEmis simulation. This slightly improves the agreement with the observation-based estimate of 11.2+/-1.3 years of Prather et al. (2012). Since the decrease in OH occurs primarily in the northern hemisphere, the NH/SH OH ratio shows a small reduction from 1.19 in the RefGMI simulation to 1.16 in the GMI-HiEmis simulation, but the large hemispheric asymmetry in OH remains.

Both the RefGMI and GMI-HiEmis simulation show a large high bias in NH TCO compared to the OMI/MLS observations, as well as a low bias in the equatorial Pacific and the extratropical SH (Figure 9). Similar biases were present in the ACCMIP multi-model mean (Young et al., 2013), indicating that these biases are a common feature in CCMs. The increased CO emissions in the GMI-HiEmis simulation slightly increase the high bias in TCO in the northern midlatitudes, but the increase is small compared to the bias in the RefGMI simulation.

Deleted: chemistry climate models

3.4 Sensitivity of OH to model biases

Given the sensitivity of the CO biases to OH (Figs. 3, 4, and 5) and the relatively small changes in OH resulting from the increased CO emissions in the GMI-HiEmis simulation, we next examine how other biases in the RefGMI simulation may impact OH concentrations and consequently the CO distribution and methane lifetime. We conducted a series of sensitivity studies using the CO-OH parameterization option to isolate the impact of several known model biases on OH and CO distributions. We analyze the results for the entire year in order to compare our results to observation-based estimates of methane lifetime.

Deleted:

The primary source of OH in the troposphere is ozone photolysis followed by reaction of O^{1}D with water vapor, and secondary production of OH occurs through reaction of HO$_2$ with NO or ozone (Spivakovsky et al., 2000). Consequently, simulated OH concentrations are sensitive to errors in NO$_x$ and ozone concentrations, water vapor, and factors that influence photolysis such as overhead ozone column and clouds. Here, we examine the sensitivity of OH to model biases in some of these factors.

3.4.1 Sensitivity to Tropospheric Ozone

Comparison of output from the CCMs that participated in the ACCMIP study to OMI/MLS TCO reveals positive biases in simulated tropospheric ozone over the NH midlatitudes, and negative biases over the tropical Pacific and SH (Young et al., 2013), which lead to an overestimate in NH OH production and an underestimate in SH OH production (Naik et al., 2013). The multi-model mean tropospheric ozone also shows a high bias in the NH and low bias in the SH compared to the Tropospheric Emission Spectrometer (TES) (Bowman et al., 2013). A multi-species assimilation study by Miyazaki et al. (2012b) found that assimilating TES ozone increased OH concentrations in the SH.

We use the CO-OH option to investigate the impact of removing the GEOSCCM's tropospheric ozone column bias relative to the OMI/MLS observations (Fig. 9). We scale the tropospheric ozone values input to the parameterization of OH for each month between October 2004 and December 2010 from 60°S-60°N so that the tropospheric ozone column is unbiased compared to the OMI/MLS TCO for that month. No scaling is applied where the TCO data is missing. We use the scaled ozone input in a sensitivity study for Oct. 2004 to Jan. 2010, called CO-OHSensTCO, which parallels the RefCO-OH

20

Deleted: O$_3$

Moved up [2]: Holmes et al. (2013) found that temperature, water vapor, stratospheric ozone, and emissions from biomass burning and lightning could together explain most of the interannual variability in methane lifetime against OH. Duncan and Logan (2008) found that changes in the ozone column were a major driver of OH variability over 1988-1997. Murray et al. (2013) found that lightning was more important for OH variability over 1998-2006, when there was less variability in the overhead ozone column. Murray et al. (2014) found that on glacial-interglacial timescales, OH concentrations were proportional to the tropospheric ozone photolysis rate, specific humidity, and reactive nitrogen emissions, and inversely proportional to CO emissions.

Deleted: s

Deleted: parameterization

simulation but uses the scaled tropospheric ozone values in the parameterization of OH. CO-OHSensTCO shows a small (2%) decrease in global mean OH compared to RefCO-OH, with a 3% decrease in NH OH and 1% decrease in SH OH. The increased OH leads to a 2% increase in both methane and methyl chloroform lifetimes against OH. The NH/SH OH ratio decreases slightly to 1.19 (Table 4), suggesting that the IHG in the tropospheric ozone bias makes only a minor contribution to the model's interhemispheric OH asymmetry.

3.4.2 Sensitivity to Stratospheric Ozone

We next examine how biases in stratospheric ozone affect OH through their role in photolysis. Voulgarakis et al. (2013) found that changes in stratospheric ozone and tropospheric OH in the ACCMIP models both correlated strongly with $J(O^1D)$. We conduct a sensitivity study for 2005 through 2009, CO-OHSensStO3, which parallels the RefCO-OH simulation but replaces the simulated ozone with the GMAO ozone assimilation in the stratosphere for input into the parameterization. The change in global mean OH in CO-OHSensStO3 is nearly identical to that of CO-OHSensTCO, but CO-OHSensStO3 places more of the change in the SH, causing the NH/SH OH ratio to increase to 1.23 (Table 4). The change in OH due to stratospheric ozone bias is small in part because GEOSCCM has relatively small biases in tropical stratospheric ozone. However, the multi-model Chemistry Climate Model Validation-2 (CCMVal-2) study (Morgenstern et al., 2010) shows a large spread across models for column ozone in the tropics (Austin et al., 2010). Thus, biases in stratospheric ozone may play a larger role in tropospheric OH in models with larger stratospheric ozone biases.

Deleted: OH

Deleted: inter-hemispheric gradient

3.4.3 Sensitivity to Water Vapor

We investigate the impact of model biases in water vapor on OH concentrations through its role in OH production. Inter-model differences in OH in the POLMIP study are correlated with inter-model differences in simulated water vapor (Monks et al., 2015). The GEOS-5 AGCM exhibits a high bias in specific humidity compared to the MERRA reanalysis in much of the troposphere (Molod et al., 2012), and a high bias in the mid-troposphere is also seen throughout the year in GEOSCCM compared to AIRS data (Lamarque et al., 2013).

We quantify the impact of this bias by conducting a sensitivity study, CO-OHSensQ, that applies altitude and latitude-dependent zonal mean scaling factors for each month to the specific humidity provided to the OH parameterization. The scaling factors are based on comparison of the RefGMI simulation to MERRA and are applied in 100 hPa intervals between 900 and 200 hPa for 60°S to 60°N. These scaling factors are designed to remove the mean bias in the simulated specific humidity compared to MERRA while allowing the simulated water vapor to vary in space and time in a manner consistent with the simulated meteorology. The water vapor scaling is applied only to the OH parameterization, and does not impact the general circulation of the simulation. The scaling results in lower specific humidity in the middle and upper troposphere, with the largest percent reductions occurring between 300 and 500 hPa (Figure 10).

Simulated OH is 6% lower in the CO-OHSensQ simulation than the RefCO-OH simulation, and the methane and methyl chloroform lifetimes against OH are thus 6% longer (Table 4). Consequently, water vapor bias has a larger impact on OH concentrations than the stratospheric or tropospheric ozone biases in our simulations.

22

The OH reduction is similar in both hemispheres in the annual mean, so the NH/SH OH gradient is unchanged compare to RefCO-OH.

3.4.4 Sensitivity to NO$_x$

Anthropogenic NO$_x$ emissions, which contribute to secondary production of OH, are located primarily in the northern hemisphere. Consequently, an overestimate of these emissions could contribute to the NH/SH asymmetry in simulated OH. Previous studies have estimated NO$_x$ emissions based on satellite observations of NO$_2$ columns (Lamsal et al., 2011; Miyazaki et al., 2012a), but some uncertainty in NO$_x$ emissions remains. We quantify the sensitivity of simulated OH to NH NO$_x$ with a sensitivity study, CO-OHSensNOx, which parallels RefCO-OH but includes 30% lower NO and NO$_2$ concentrations in the NH. We note that in this experiment, ozone values remain the same as in RefCO-OH, rather than responding to the change in NO$_x$. The reduction in NH NO$_x$ emissions leads to a 3% reduction in global OH (Table 4). SH and NH OH are reduced by 0.3% and 6%, respectively, reducing the NH/SH OH ratio to 1.15. While this shows that the hemispheric asymmetry in OH is affected by NO$_x$ emissions, a much larger redistribution of NO$_x$ emissions would be required to completely eliminate the asymmetry.

3.4.5 Summary of OH Sensitivities

In the previous sections, we examined the sensitivity of OH and its IHG to model biases in tropospheric and stratospheric ozone, water vapor, and NH NO$_x$ emissions. We find that water vapor has the largest impact on global mean OH, while NH NO$_x$ emissions have the largest impact on the NH/SH ratio. However, none of these biases

23

individually explains the 20% reduction in NH OH that would remove the interhemispheric asymmetry and which Figures 4 and 5 suggest are necessary to remove most of the CO bias. We note, however, that the CO-OH option simulations do not account for all the chemical feedbacks between ozone, methane, OH, and other species, and may underestimate the sensitivity of the full chemistry simulation to some of these biases.

Table 4 suggests that applying multiple bias corrections simultaneously would bring our simulation into good agreement with the observation-based estimates of global mean OH. We conduct a final sensitivity simulation, called CO-OHSensAll, incorporating the bias corrections for tropospheric and stratospheric ozone, as well as the specific humidity scaling and 30% reduction in NH NO_x emissions. This simulation results in a 13% reduction in global mean OH, with a 10% reduction in the SH and 16% reduction in the NH. The NH/SH OH ratio is reduced to 1.14. The lifetimes of methyl chloroform and methane in this simulation increase by 15%. Applying this 15% increase in methane lifetime to the RefGMI methane lifetime against OH of 9.6 years would yield a lifetime of 11 years, consistent with the 11.2+/-1.3 year estimate of Prather et al. (2012). This shows that removing the main model biases related to OH production would bring simulated global mean OH into good agreement with observation-based estimates, although some NH/SH asymmetry would remain.

The reduction in OH in the sensitivity studies compared to RefCO-OH leads to higher surface concentrations of CO. The bias in the global mean March through August surface CO changes from -4% in RefCO-OH to 3% in CO-OHSensAll, while the bias in the IHG changes from -11% to -4%. Figure 11 shows the latitudinal distribution of the

24

change in CO for each sensitivity simulation versus RefCO-OH. The sum of the changes for CO-OHSensTCO, CO-OHSensStO3, CO-OHSensQ, and CO-OHSensNOx, shown in the dotted line, is similar but slightly smaller than the change for CO-OHSensAll, indicating small non-linearities in the system. Correcting water vapor (CO-OHSensQ) makes a large contribution to the CO enhancement in both hemispheres, while adjusting NO_x emissions (CO-OHSensNOx) and to a lesser extent tropospheric ozone (CO-OHSensTCO) contributes to the larger increase in the northern hemisphere.

4 Conclusions

We examined possible causes of CO model bias, such as underestimated emissions or overestimated OH, in a global CCM. An underestimate of CO emissions can impact the chemistry-climate simulation through the interaction of CO with methane via OH and with ozone, but we find the effects to be small. In contrast, a CO bias due to excess OH would imply biases in methane lifetime, further influencing the simulated climate.

Either increasing emissions or decreasing northern hemisphere OH can remove the bias in the latitudinal gradient of CO compared to surface observations. However, we find that the large increases in Asian anthropogenic emissions needed to remove the negative CO bias at remote surface sites leads to overestimates of CO over Asia compared to MOPITT. In contrast, reducing OH in the northern hemisphere improves the agreement between simulated and observed CO concentrations. This is consistent with the finding of Patra et al. (2014) that the ratio of northern hemisphere to southern hemisphere OH is close to one. We note that biases in OH, CO emissions, and transport are not mutually exclusive, and the model bias in CO is likely influenced by a combination of these factors.

25

Deleted: chemistry climate model

Deleted: concentrations

Deleted: concentrations

The availability of satellite-based constraints on CO, ozone, and water vapor enables us to assess model biases that affect the major sources and sinks of OH and hence CO concentrations and methane lifetime. We used a CO-OH parameterization to explore the effect of model biases in ozone and water vapor on simulated OH and CO. Removing the high bias in northern hemisphere tropospheric ozone, a common feature of CCMs, had only a small effect on simulated OH and methane lifetime. A high bias in water vapor had a larger impact on global mean OH, but removing this bias did not remove the northern versus southern hemisphere asymmetry in OH. Removing both ozone and water vapor biases, as well as decreasing northern hemisphere NO_x, provided the desired increase in methane lifetime, but was insufficient to remove the hemispheric asymmetry in OH. Thus, while a NH/SH OH ratio near one improves the simulation of CO, we cannot generate this ratio in our simulations by removing known model biases in ozone and water vapor.

Our study suggests that the springtime low bias in CO at northern latitudes often seen in CCM simulations likely indicates a bias in methane lifetime. Improving the model representation of water vapor and ozone, as well as reducing uncertainty in NO_x emissions, could reduce these biases. However, additional research is needed to understand the causes of northern versus southern asymmetry in simulated OH. Future field missions that provide data on the latitudinal distribution of CO and oxidant sources and losses will be valuable for understanding biases in simulated CO and OH.

Acknowledgements

26

Deleted: O_3

Deleted: concentrations

Deleted: CH_4

Deleted: CH_4

Deleted: chemistry climate model
Deleted: CH_4

27

1 **References**

2 Arellano, A. F., and Hess, P. G.: Sensitivity of top-down estimates of CO sources to

3 GCTM transport, Geophysical Research Letters, 33, 10.1029/2006gl027371, 2006.

4 Austin, J., Scinocca, J., Plummer, D., Oman, L., Waugh, D., Akiyoshi, H., Bekki, S.,

5 Braesicke, P., Butchart, N., Chipperfield, M., Cugnet, D., Dameris, M., Dhomse, S.,

6 Eyring, V., Frith, S., Garcia, R. R., Garny, H., Gettelman, A., Hardiman, S. C., Kinnison,

7 D., Lamarque, J. F., Mancini, E., Marchand, M., Michou, M., Morgenstern, O.,

8 Nakamura, T., Pawson, S., Pitari, G., Pyle, J., Rozanov, E., Shepherd, T. G., Shibata, K.,

9 Teyssedre, H., Wilson, R. J., and Yamashita, Y.: Decline and recovery of total column

10 ozone using a multimodel time series analysis, Journal of Geophysical Research-

11 Atmospheres, 115, 10.1029/2010jd013857, 2010.

12 Berntsen, T. K., Fuglestvedt, J. S., Joshi, M. M., Shine, K. P., Stuber, N., Ponater, M.,

13 Sausen, R., Hauglustaine, D. A., and Li, L.: Response of climate to regional emissions of

14 ozone precursors: sensitivities and warming potentials, Tellus Series B-Chemical and

15 Physical Meteorology, 57, 283-304, 10.1111/j.1600-0889.2005.00152.x, 2005.

16 Bian, H. S., Chin, M. A., Kawa, S. R., Yu, H. B., Diehl, T., and Kucsera, T.: Multiscale

17 carbon monoxide and aerosol correlations from satellite measurements and the GOCART

18 model: Implication for emissions and atmospheric evolution, Journal of Geophysical

19 Research-Atmospheres, 115, 14, 10.1029/2009jd012781, 2010.

20 Bloom, S. C., Takacs, L. L., da Silva, A. M., and Ledvina, D.: Data Assimilation Using

21 Incremental Analysis Updates, Monthly Weather Review, 124, 1256-1271,

22 10.1175/1520-0493(1996)124<1256:DAUIAU>2.0.CO;2, 1996.

28

1 Bowman, K., and Henze, D. K.: Attribution of direct ozone radiative forcing to spatially

2 resolved emissions, Geophysical Research Letters, 39, 10.1029/2012gl053274, 2012.

3 Bowman, K. W., Shindell, D. T., Worden, H. M., Lamarque, J. F., Young, P. J.,

4 Stevenson, D. S., Qu, Z., de la Torre, M., Bergmann, D., Cameron-Smith, P. J., Collins,

5 W. J., Doherty, R., Dalsoren, S. B., Faluvegi, G., Folberth, G., Horowitz, L. W., Josse, B.

6 M., Lee, Y. H., MacKenzie, I. A., Myhre, G., Nagashima, T., Naik, V., Plummer, D. A.,

7 Rumbold, S. T., Skeie, R. B., Strode, S. A., Sudo, K., Szopa, S., Voulgarakis, A., Zeng,

8 G., Kulawik, S. S., Aghedo, A. M., and Worden, J. R.: Evaluation of ACCMIP outgoing

9 longwave radiation from tropospheric ozone using TES satellite observations,

10 Atmospheric Chemistry and Physics, 13, 4057-4072, 10.5194/acp-13-4057-2013, 2013.

11 Daniel, J. S., and Solomon, S.: On the climate forcing of carbon monoxide, Journal of

12 Geophysical Research-Atmospheres, 103, 13249-13260, 10.1029/98jd00822, 1998.

13 Deeter, M. N., Worden, H. M., Gille, J. C., Edwards, D. P., Mao, D., and Drummond, J.

14 R.: MOPITT multispectral CO retrievals: Origins and effects of geophysical radiance

15 errors, Journal of Geophysical Research-Atmospheres, 116, 10.1029/2011jd015703,

16 2011.

17 Deeter, M. N., Martinez-Alonso, S., Edwards, D. P., Emmons, L. K., Gille, J. C.,

18 Worden, H. M., Pittman, J. V., Daube, B. C., and Wofsy, S. C.: Validation of MOPITT

19 Version 5 thermal-infrared, near-infrared, and multispectral carbon monoxide profile

20 retrievals for 2000-2011, Journal of Geophysical Research-Atmospheres, 118, 6710-

21 6725, 10.1002/jgrd.50272, 2013.

29

1 Derwent, R. G., Collins, W. J., Johnson, C. E., and Stevenson, D. S.: Transient behaviour

2 of tropospheric ozone precursors in a global 3-D CTM and their indirect greenhouse

3 effects, Climatic Change, 49, 463-487, 10.1023/a:1010648913655, 2001.

4 Duncan, B., Portman, D., Bey, I., and Spivakovsky, C.: Parameterization of OH for

5 efficient computation in chemical tracer models, Journal of Geophysical Research-

6 Atmospheres, 105, 12259-12262, 10.1029/1999jd901141, 2000.

7 Duncan, B. N., Logan, J. A., Bey, I., Megretskaia, I. A., Yantosca, R. M., Novelli, P. C.,

8 Jones, N. B., and Rinsland, C. P.: Global budget of CO, 1988-1997: Source estimates and

9 validation with a global model, Journal of Geophysical Research-Atmospheres, 112,

10 10.1029/2007jd008459, 2007a.

11 Duncan, B. N., Strahan, S. E., Yoshida, Y., Steenrod, S. D., and Livesey, N.: Model study

12 of the cross-tropopause transport of biomass burning pollution, Atmospheric Chemistry

13 and Physics, 7, 3713-3736, 2007b.

14 Duncan, B. N., and Logan, J. A.: Model analysis of the factors regulating the trends and

15 variability of carbon monoxide between 1988 and 1997, Atmospheric Chemistry and

16 Physics, 8, 7389-7403, 2008.

17 Edwards, D. P., Emmons, L. K., Hauglustaine, D. A., Chu, D. A., Gille, J. C., Kaufman,

18 Y. J., Petron, G., Yurganov, L. N., Giglio, L., Deeter, M. N., Yudin, V., Ziskin, D. C.,

19 Warner, J., Lamarque, J. F., Francis, G. L., Ho, S. P., Mao, D., Chen, J., Grechko, E. I.,

20 and Drummond, J. R.: Observations of carbon monoxide and aerosols from the Terra

21 satellite: Northern Hemisphere variability, Journal of Geophysical Research-

22 Atmospheres, 109, 10.1029/2004jd004727, 2004.

30

Emmons, L. K., Deeter, M. N., Gille, J. C., Edwards, D. P., Attie, J. L., Warner, J., Ziskin, D., Francis, G., Khattatov, B., Yudin, V., Lamarque, J. F., Ho, S. P., Mao, D., Chen, J. S., Drummond, J., Novelli, P., Sachse, G., Coffey, M. T., Hannigan, J. W., Gerbig, C., Kawakami, S., Kondo, Y., Takegawa, N., Schlager, H., Baehr, J., and Ziereis, H.: Validation of Measurements of Pollution in the Troposphere (MOPITT) CO retrievals with aircraft in situ profiles, Journal of Geophysical Research-Atmospheres, 109, 10.1029/2003jd004101, 2004.

Fortems-Cheiney, A., Chevallier, F., Pison, I., Bousquet, P., Szopa, S., Deeter, M. N., and Clerbaux, C.: Ten years of CO emissions as seen from Measurements of Pollution in the Troposphere (MOPITT), Journal of Geophysical Research-Atmospheres, 116, 10.1029/2010jd014416, 2011.

Fry, M. M., Naik, V., West, J. J., Schwarzkopf, M. D., Fiore, A. M., Collins, W. J., Dentener, F. J., Shindell, D. T., Atherton, C., Bergmann, D., Duncan, B. N., Hess, P., MacKenzie, I. A., Marmer, E., Schultz, M. G., Szopa, S., Wild, O., and Zeng, G.: The influence of ozone precursor emissions from four world regions on tropospheric composition and radiative climate forcing, Journal of Geophysical Research-Atmospheres, 117, 10.1029/2011jd017134, 2012.

Fry, M. M., Schwarzkopf, M. D., Adelman, Z., Naik, V., Collins, W. J., and West, J. J.: Net radiative forcing and air quality responses to regional CO emission reductions, Atmospheric Chemistry and Physics, 13, 5381-5399, 10.5194/acp-13-5381-2013, 2013.

Fuglestvedt, J. S., Isaksen, I. S. A., and Wang, W. C.: Estimates of indirect global warming potentials for CH4, CO AND NOX, Climatic Change, 34, 405-437, 10.1007/bf00139300, 1996.

Holloway, T., Levy, H., and Kasibhatla, P.: Global distribution of carbon monoxide, Journal of Geophysical Research-Atmospheres, 105, 12123-12147, 10.1029/1999jd901173, 2000.

Holmes, C. D., Prather, M. J., Sovde, O. A., and Myhre, G.: Future methane, hydroxyl, and their uncertainties: key climate and emission parameters for future predictions, Atmospheric Chemistry and Physics, 13, 285-302, 10.5194/acp-13-285-2013, 2013.

Hooghiemstra, P. B., Krol, M. C., Meirink, J. F., Bergamaschi, P., van der Werf, G. R., Novelli, P. C., Aben, I., and Rockmann, T.: Optimizing global CO emission estimates using a four-dimensional variational data assimilation system and surface network observations, Atmospheric Chemistry and Physics, 11, 4705-4723, 10.5194/acp-11-4705-2011, 2011.

IPCC: Climate Change: The IPCC Scientific Assessment, J.T. Houghton, G.J. Jenkins and J.J. Ephraums (eds.), Cambridge University Press, 1990.

Johnson, C. E., and Derwent, R. G.: Relative radiative forcing consequences of global emissions of hydrocarbons, carbon monoxide and NOx from human activities estimated with a zonally-averaged two-dimensional model, Climatic Change, 34, 439-462, 10.1007/bf00139301, 1996.

Jones, D. B. A., Bowman, K. W., Logan, J. A., Heald, C. L., Liu, J., Luo, M., Worden, J., and Drummond, J.: The zonal structure of tropical O-3 and CO as observed by the Tropospheric Emission Spectrometer in November 2004-Part 1: Inverse modeling of CO emissions, Atmospheric Chemistry and Physics, 9, 3547-3562, 2009.

Kopacz, M., Jacob, D. J., Fisher, J. A., Logan, J. A., Zhang, L., Megretskaia, I. A., Yantosca, R. M., Singh, K., Henze, D. K., Burrows, J. P., Buchwitz, M., Khlystova, I.,

McMillan, W. W., Gille, J. C., Edwards, D. P., Eldering, A., Thouret, V., and Nedelec, P.: Global estimates of CO sources with high resolution by adjoint inversion of multiple satellite datasets (MOPITT, AIRS, SCIAMACHY, TES), Atmospheric Chemistry and Physics, 10, 855-876, 2010.

Lamarque, J. F., Shindell, D. T., Josse, B., Young, P. J., Cionni, I., Eyring, V., Bergmann, D., Cameron-Smith, P., Collins, W. J., Doherty, R., Dalsoren, S., Faluvegi, G., Folberth, G., Ghan, S. J., Horowitz, L. W., Lee, Y. H., MacKenzie, I. A., Nagashima, T., Naik, V., Plummer, D., Righi, M., Rumbold, S. T., Schulz, M., Skeie, R. B., Stevenson, D. S., Strode, S., Sudo, K., Szopa, S., Voulgarakis, A., and Zeng, G.: The Atmospheric Chemistry and Climate Model Intercomparison Project (ACCMIP): overview and description of models, simulations and climate diagnostics, Geoscientific Model Development, 6, 179-206, 10.5194/gmd-6-179-2013, 2013.

Lamsal, L. N., Martin, R. V., Padmanabhan, A., van Donkelaar, A., Zhang, Q., Sioris, C. E., Chance, K., Kurosu, T. P., and Newchurch, M. J.: Application of satellite observations for timely updates to global anthropogenic NO_x emission inventories, Geophysical Research Letters, 38(L05810), doi:10.1029/2010GL046476, 2011.

Logan, J. A., Prather, M. J., Wofsy, S. C., and McElroy, M. B.: Tropospheric Chemistry: A global Perspective, Journal of Geophysical Research-Atmospheres, 86(C8), 7210-7254, 1981.

Mao, J., Fan, S., Jacob, D. J., and Travis, K. R.: Radical loss in the atmosphere from Cu-Fe redox coupling in aerosols, Atmospheric Chemistry and Physics, 13, 509-519, 10.5194/acp-13-509-2013, 2013.

33

Miyazaki, K., Eskes, H. J., Sudo, K.: Global NO_x emission estimates derived from an assimilation of OMI tropospheric NO_2 columns, Atmospheric Chemistry and Physics, 12, 2263-2288, 10.5194/acp-12-2263-2012, 2012a.

Miyazaki, K., Eskes, H. J., Sudo, K., Takigawa, M., van Weele, M., and Boersma, K. F.: Simultaneous assimilation of satellite NO2, O-3, CO, and HNO3 data for the analysis of tropospheric chemical composition and emissions, Atmospheric Chemistry and Physics, 12, 9545-9579, 10.5194/acp-12-9545-2012, 2012b.

Molod, A., Takacs, L., Suarez, M., Bacmeister, J., Song, I.-S., and Eichmann, A.: The GEOS-5 atmospheric general circulation model: Mean climate and development from MERRA to Fortuna, NASA, Goddard Space Flight Center, Greenbelt, MD, 2012.

Monks, S. A., Arnold, S. R., Emmons, L. K., Law, K. S., Turquety, S., Duncan, B. N., Flemming, J., Huijnen, V., Tilmes, S., Langner, J., Mao, J., Long, Y., Thomas, J. L., Steenrod, S. D., Raut, J. C., Wilson, C., Chipperfield, M. P., Diskin, G. S., Weinheimer, A., Schlager, H., and Ancellet, G.: Multi-model study of chemical and physical controls on transport of anthropogenic and biomass burning pollution to the Arctic, Atmos. Chem. Phys., 15, 3575-3603, 10.5194/acp-15-3575-2015, 2015.

Morgenstern, O., Giorgetta, M. A., Shibata, K., Eyring, V., Waugh, D. W., Shepherd, T. G., Akiyoshi, H., Austin, J., Baumgaertner, A. J. G., Bekki, S., Braesicke, P., Bruhl, C., Chipperfield, M. P., Cugnet, D., Dameris, M., Dhomse, S., Frith, S. M., Garny, H., Gettelman, A., Hardiman, S. C., Hegglin, M. I., Jockel, P., Kinnison, D. E., Lamarque, J. F., Mancini, E., Manzini, E., Marchand, M., Michou, M., Nakamura, T., Nielsen, J. E., Olivie, D., Pitari, G., Plummer, D. A., Rozanov, E., Scinocca, J. F., Smale, D., Teyssedre, H., Toohey, M., Tian, W., and Yamashita, Y.: Review of the formulation of present-

34

generation stratospheric chemistry-climate models and associated external forcings, Journal of Geophysical Research-Atmospheres, 115, 10.1029/2009jd013728, 2010.

Muller, J. F., and Stavrakou, T.: Inversion of CO and NOx emissions using the adjoint of the IMAGES model, Atmospheric Chemistry and Physics, 5, 1157-1186, 2005.

Murray, L. T., Logan, J. A., and Jacob, D. J.: Interannual variability in tropical tropospheric ozone and OH: The role of lightning, Journal of Geophysical Research-Atmospheres, 118, 11468-11480, 10.1002/jgrd.50857, 2013.

Murray, L. T., Mickley, L. J., Kaplan, J. O., Sofen, E. D., Pfeiffer, M., and Alexander, B.: Factors controlling variability in the oxidative capacity of the troposphere since the Last Glacial Maximum, Atmos. Chem. Phys., 14, 3589-3622, 10.5194/acp-14-3589-2014, 2014.

Naik, V., Mauzerall, D., Horowitz, L., Schwarzkopf, M. D., Ramaswamy, V., and Oppenheimer, M.: Net radiative forcing due to changes in regional emissions of tropospheric ozone precursors, Journal of Geophysical Research-Atmospheres, 110, 10.1029/2005jd005908, 2005.

Naik, V., Voulgarakis, A., Fiore, A. M., Horowitz, L. W., Lamarque, J. F., Lin, M., Prather, M. J., Young, P. J., Bergmann, D., Cameron-Smith, P. J., Cionni, I., Collins, W. J., Dalsoren, S. B., Doherty, R., Eyring, V., Faluvegi, G., Folberth, G. A., Josse, B., Lee, Y. H., MacKenzie, I. A., Nagashima, T., van Noije, T. P. C., Plummer, D. A., Righi, M., Rumbold, S. T., Skeie, R., Shindell, D. T., Stevenson, D. S., Strode, S., Sudo, K., Szopa, S., and Zeng, G.: Preindustrial to present-day changes in tropospheric hydroxyl radical and methane lifetime from the Atmospheric Chemistry and Climate Model

Intercomparison Project (ACCMIP), Atmospheric Chemistry and Physics, 13, 5277-5298, 10.5194/acp-13-5277-2013, 2013.

Novelli, P. C., and Masarie, K. A.: Atmospheric Carbon Monoxide Dry Air Mole Fractions from the NOAA ESRL Carbon Cycle Cooperative Global Air Sampling Network, 1988-2013, Version: 2014-07-02, Path: ftp://aftp.cmdl.noaa.gov/data/trace_gases/co/flask/surface/, 2014.

Patra, P. K., Krol, M. C., Montzka, S. A., Arnold, T., Atlas, E. L., Lintner, B. R., Stephens, B. B., Xiang, B., Elkins, J. W., Fraser, P. J., Ghosh, A., Hintsa, E. J., Hurst, D. F., Ishijima, K., Krummel, P. B., Miller, B. R., Miyazaki, K., Moore, F. L., Muhle, J., O/'Doherty, S., Prinn, R. G., Steele, L. P., Takigawa, M., Wang, H. J., Weiss, R. F., Wofsy, S. C., and Young, D.: Observational evidence for interhemispheric hydroxyl-radical parity, Nature, 513, 219-223, 10.1038/nature13721, 2014.

Petron, G., Granier, C., Khattatov, B., Yudin, V., Lamarque, J. F., Emmons, L., Gille, J., and Edwards, D. P.: Monthly CO surface sources inventory based on the 2000-2001 MOPITT satellite data, Geophysical Research Letters, 31, 10.1029/2004gl020560, 2004.

Pison, I., Bousquet, P., Chevallier, F., Szopa, S., and Hauglustaine, D.: Multi-species inversion of CH4, CO and H-2 emissions from surface measurements, Atmospheric Chemistry and Physics, 9, 5281-5297, 2009.

Prather, M. J.: Time scales in atmospheric chemistry: Theory, GWPs for CH_4 and CO, and runaway growth, Geophysical Research Letters, 23, 2597-2600, 1996.

Prather, M. J., Holmes, C. D., and Hsu, J.: Reactive greenhouse gas scenarios: Systematic exploration of uncertainties and the role of atmospheric chemistry, Geophysical Research Letters, 39, 10.1029/2012gl051440, 2012.

36

Prinn, R. G., Huang, J., Weiss, R. F., Cunnold, D. M., Fraser, P. J., Simmonds, P. G., McCulloch, A., Harth, C., Reimann, S., Salameh, P., O'Doherty, S., Wang, R. H. J., Porter, L. W., Miller, B. R., and Krummel, P. B.: Evidence for variability of atmospheric hydroxyl radicals over the past quarter century, Geophysical Research Letters, 32, 10.1029/2004gl022228, 2005.

Rienecker, M. M., Suarez, M. J., Gelaro, R., Todling, R., Bacmeister, J., Liu, E., Bosilovich, M. G., Schubert, S. D., Takacs, L., Kim, G.-K., Bloom, S., Chen, J., Collins, D., Conaty, A., da Silva, A., Gu, W., Joiner, J., Koster, R. D., Lucchesi, R., Molod, A., Owens, T., Pawson, S., Pegion, P., Redder, C. R., Reichle, R., Robertson, F. R., Ruddick, A. G., Sienkiewicz, M., and Woollen, J.: MERRA: NASA's Modern-Era Retrospective Analysis for Research and Applications, Journal of Climate, 24, 3624-3648, 10.1175/JCLI-D-11-00015.1, 2011.

Rohrer, F., and Berresheim, H.: Strong correlation between levels of tropospheric hydroxyl radicals and solar ultraviolet radiation, Nature, 442, 184-187, http://www.nature.com/nature/journal/v442/n7099/suppinfo/nature04924_S1.html, 2006.

Shindell, D. T., Faluvegi, G., Stevenson, D. S., Krol, M. C., Emmons, L. K., Lamarque, J. F., Petron, G., Dentener, F. J., Ellingsen, K., Schultz, M. G., Wild, O., Amann, M., Atherton, C. S., Bergmann, D. J., Bey, I., Butler, T., Cofala, J., Collins, W. J., Derwent, R. G., Doherty, R. M., Drevet, J., Eskes, H. J., Fiore, A. M., Gauss, M., Hauglustaine, D. A., Horowitz, L. W., Isaksen, I. S. A., Lawrence, M. G., Montanaro, V., Muller, J. F., Pitari, G., Prather, M. J., Pyle, J. A., Rast, S., Rodriguez, J. M., Sanderson, M. G., Savage, N. H., Strahan, S. E., Sudo, K., Szopa, S., Unger, N., van Noije, T. P. C., and Zeng, G.: Multimodel simulations of carbon monoxide: Comparison with observations

and projected near-future changes, Journal of Geophysical Research-Atmospheres, 111, 10.1029/2006jd007100, 2006.

Shindell, D. T., Faluvegi, G., Koch, D. M., Schmidt, G. A., Unger, N., and Bauer, S. E.: Improved Attribution of Climate Forcing to Emissions, Science, 326, 716-718, 10.1126/science.1174760, 2009.

Spivakovsky, C. M., Logan, J. A., Montzka, S. A., Balkanski, Y. J., Foreman-Fowler, M., Jones, D. B. A., Horowitz, L. W., Fusco, A. C., Brenninkmeijer, C. A. M., Prather, M. J., Wofsy, S. C., and McElroy, M. B.: Three-dimensional climatological distribution of tropospheric OH: Update and evaluation, Journal of Geophysical Research-Atmospheres, 105, 8931-8980, 10.1029/1999jd901006, 2000.

Stein, O., Schultz, M. G., Bouarar, I., Clark, H., Huijnen, V., Gaudel, A., George, M., and Clerbaux, C.: On the wintertime low bias of Northern Hemisphere carbon monoxide found in global model simulations, Atmospheric Chemistry and Physics, 14, 9295-9316, 10.5194/acp-14-9295-2014, 2014.

Strahan, S. E., Duncan, B. N., and Hoor, P.: Observationally derived transport diagnostics for the lowermost stratosphere and their application to the GMI chemistry and transport model, Atmospheric Chemistry and Physics, 7, 2435-2445, 2007.

Strode, S. A., and Pawson, S.: Detection of carbon monoxide trends in the presence of interannual variability, Journal of Geophysical Research-Atmospheres, 118, 12257-12273, 10.1002/2013JD020258, 2013.

Voulgarakis, A., Naik, V., Lamarque, J. F., Shindell, D. T., Young, P. J., Prather, M. J., Wild, O., Field, R. D., Bergmann, D., Cameron-Smith, P., Cionni, I., Collins, W. J., Dalsøren, S. B., Doherty, R. M., Eyring, V., Faluvegi, G., Folberth, G. A., Horowitz, L.

38

W., Josse, B., MacKenzie, I. A., Nagashima, T., Plummer, D. A., Righi, M., Rumbold, S.

T., Stevenson, D. S., Strode, S. A., Sudo, K., Szopa, S., and Zeng, G.: Analysis of present

day and future OH and methane lifetime in the ACCMIP simulations, Atmos. Chem.

Phys., 13, 2563-2587, 10.5194/acp-13-2563-2013, 2013.

Wargan, K., Pawson, S., Olsen, M. A., Witte, J. C., Douglass, A. R., Ziemke, J. R.,

Strahan, S. E., and Nielsen, J. E.: The global structure of upper troposphere-lower

stratosphere ozone in GEOS-5: A multiyear assimilation of EOS Aura data, Journal of

Geophysical Research: Atmospheres, 120, 2014JD022493, 10.1002/2014JD022493,

2015.

Young, P. J., Archibald, A. T., Bowman, K. W., Lamarque, J. F., Naik, V., Stevenson, D.

S., Tilmes, S., Voulgarakis, A., Wild, O., Bergmann, D., Cameron-Smith, P., Cionni, I.,

Collins, W. J., Dalsoren, S. B., Doherty, R. M., Eyring, V., Faluvegi, G., Horowitz, L.

W., Josse, B., Lee, Y. H., MacKenzie, I. A., Nagashima, T., Plummer, D. A., Righi, M.,

Rumbold, S. T., Skeie, R. B., Shindell, D. T., Strode, S. A., Sudo, K., Szopa, S., and

Zeng, G.: Pre-industrial to end 21st century projections of tropospheric ozone from the

Atmospheric Chemistry and Climate Model Intercomparison Project (ACCMIP),

Atmospheric Chemistry and Physics, 13, 2063-2090, 10.5194/acp-13-2063-2013, 2013.

Ziemke, J. R., Chandra, S., Labow, G. J., Bhartia, P. K., Froidevaux, L., and Witte, J. C.:

A global climatology of tropospheric and stratospheric ozone derived from Aura OMI

and MLS measurements, Atmospheric Chemistry and Physics, 11, 9237-9251,

10.5194/acp-11-9237-2011, 2011.

Ziemke, J. R., Olsen, M. A., Witte, J. C., Douglass, A. R., Strahan, S. E., Wargan, K.,

Liu, X., Schoeberl, M. R., Yang, K., Kaplan, T. B., Pawson, S., Duncan, B. N., Newman,

1   P. A., Bhartia, P. K., and Heney, M. K.: Assessment and applications of NASA ozone

2   data products derived from Aura OMI/MLS satellite measurements in context of the GMI

3   chemical transport model, Journal of Geophysical Research-Atmospheres, 119, 5671-

4   5699, 10.1002/2013jd020914, 2014.

5

6

7

1 **Table 1:** Description of reference and sensitivity simulations used in this study with each chemistry option

Simulation	Description	Key Result
GMI chemistry simulations		
RefGMI*	ACCMIP timeslice simulation for 2000	CO biased low at high latitudes
GMI-HiEmis	increased CO emissions compared to RefGMI	Regional CO biases compared to MOPITT
CO-only simulations		
RefCOonly*	Tagged-CO version of RefGMI	Similar CO biases to RefGMI
COonlyLowNHOH	NH OH uniformly decreased by 20%	Improves agreement with GMD CO observations
COonlySD	meteorology constrained by MERRA (specified dynamics)	Improves agreement with GMD CO observations in summer
CO-OH simulations		
RefCO-OH*	Parameterized OH version of RefGMI	Lower OH than RefGMI
CO-OHSensTCO	tropospheric ozone column adjusted to match OMI/MLS TCO	2.5% increase in CH$_4$ lifetime
CO-OHSensStO3	stratospheric O$_3$ adjusted to match assimilated O$_3$	2.4% increase in CH$_4$ lifetime
CO-OHSensQ	tropospheric water vapor adjusted based on MERRA	5.7% increase in CH$_4$ lifetime
CO-OHSensNOx	30% decrease in NH NO$_x$ concentrations	3.5% increase in CH$_4$ lifetime; OH asymmetry reduced but not eliminated
CO-OHSensAll	tropospheric and stratospheric O$_3$, water vapor, and NH NO$_x$ all adjusted	15% increase in CH$_4$ lifetime; OH asymmetry reduced but not eliminated

2
3
4
*Reference simulation

41

Deleted: Small

Deleted: Small

Deleted: I

Deleted: Small

1   **Table 2:** Tropospheric OH concentrations and lifetimes against oxidation by tropospheric

2   OH

	RefGMI	GMI-HiEmis	RefCO-OH
Global Mean OH (10^6 molec cm^{-3})	1.14	1.11	1.05
SH OH (10^6 molec cm^{-3})	1.03	1.02	0.943
NH OH (10^6 molec cm^{-3})	1.22	1.18	1.15
NH/SH OH	1.19	1.16	1.22
CH$_4$ lifetime (years)	9.65	9.89	10.5
CH$_3$CCl$_3$ lifetime (years)	5.91	6.06	6.39

3

4

5

1 **Table 3**: CO emission adjustment for the high emission simulation compared to the

2 standard simulation

Emission Increase (%)	Months			
	Jan.-Feb.	March-May	June-Aug.	Sept.-Dec.
Asian & European anthropogenic; Russian BB	17.4	45.0	63.2	0.00
Tropical BB	26.4	60.6	28.2	0.00

3
4

5

1 **Table 4:** NH/SH OH ratio and percent changes in tropospheric OH concentrations and

2 lifetimes against tropospheric OH for the CO-OH sensitivity studies compared to the

3 RefCO-OH simulation

	SensTCO	SensStO3	SensQ	SensNOx	SensAll
NH/SH OH	1.19	1.23	1.22	1.15	1.14
% change vs. RefCO-OH					
Global Mean OH	-2.1	-2.1	-6.2	-3.1	-13
SH OH	-1	-2.9	-6.3	-0.3	-10
NH OH	-3.1	-1.5	-6.1	-5.7	-16
CH_4 lifetime	2.5	2.4	5.7	3.5	15
CH_3CCl_3 lifetime	2.4	2.3	5.9	3.5	15

4

5

6

44
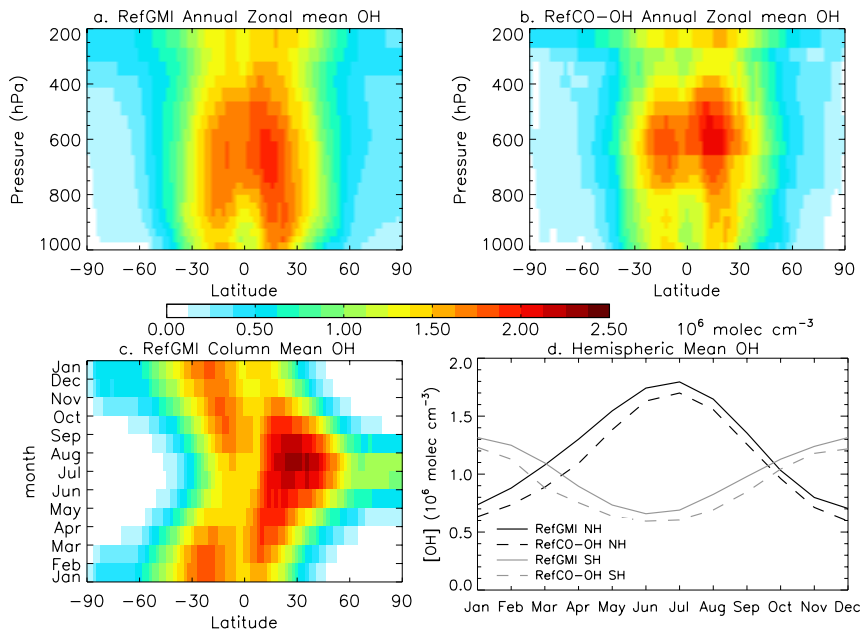
1

2

3 **Figure 1: Simulated annual zonal mean OH concentration for the RefGMI (a) and**

4 **RefCO-OH simulations (b) averaged over 1999-2009. c) The annual cycle of the**

5 **pressure-weighted column mean OH by latitude from the RefGMI simulation. The**

6 **column is averaged between the surface and 200 hPa. d) The annual cycle of**

7 **hemispheric mean OH from the RefGMI (solid lines) and RefCO-OH (dashed lines)**

8 **simulations for the northern hemisphere (black lines) and southern hemisphere**

9 **(gray lines).**

10

11

1
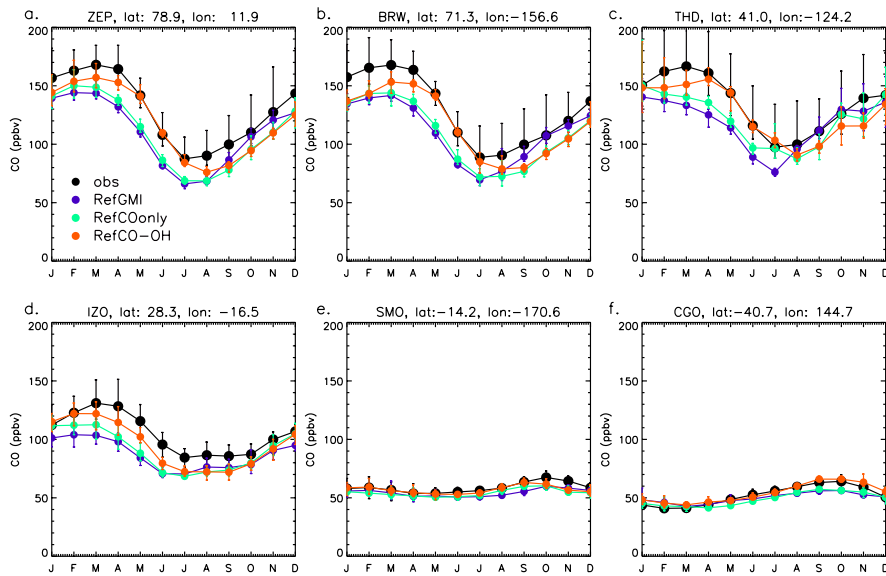
Figure 2: Monthly mean GMD observations (black) and results from the RefGMI (purple), RefCOonly (green), and RefCO-OH (orange) simulations. Circles and error bars represent the mean and min-max range, respectively, for 1999-2009. The GMD sites are as follows: a.) Ny-Alesund, Svalbard (ZEP, 78.9°N, 11.9°E), b.) Barrow, Alaska (BRW, 71.3°N, 156.6°W), c.) Trinidad Head, California (THD, 41.0°N, 124.2°W), d.) Izana, Tenerife, Canary Islands (IZO, 28.3°N, 16.5°W), Tutuila, American Samoa (SMO, 14.2°S, 170.6°W), and e.) Cape Grim, Tasmania (CGO, 40.7°S, 144.7°E).

1
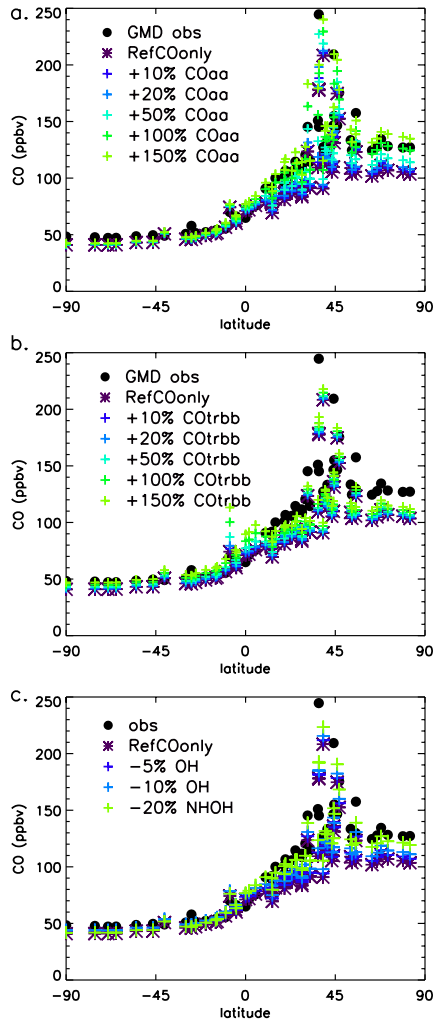
Figure 3: Latitudinal distribution of CO observations from the GMD network (black circles) and simulated CO from the RefCOonly simulation (purple stars) averaged over March-Aug. Blue-green + signs indicate the effect of a) increasing the Asian anthropogenic CO tracer, b) increasing the tropical biomass burning CO tracer, and c) decreasing OH globally by 5 or 10%, or decreasing NH OH by 20%.

1
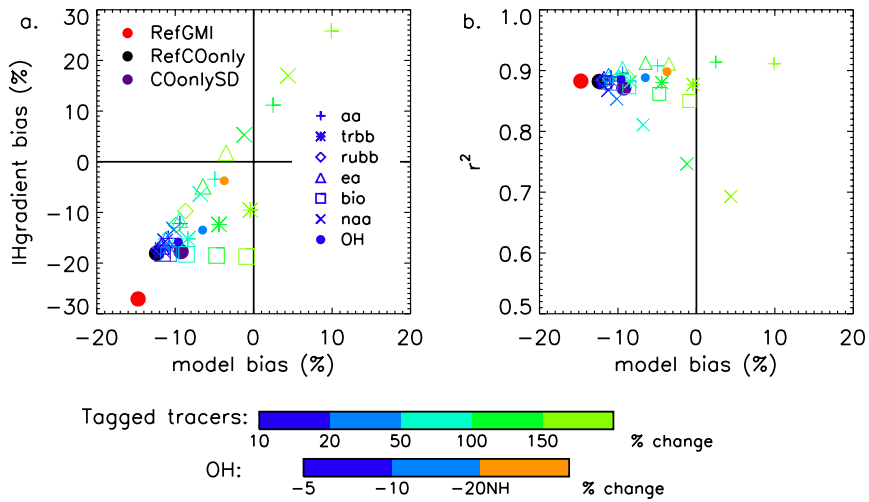
Figure 4: The impact of increasing the tagged CO tracers for Asian anthropogenic (+), tropical biomass burning (star), Russian biomass burning (diamonds), European anthropogenic (triangles), biogenic (squares), and North American anthropogenic (x) sources on a) bias in the inter-hemispheric gradient versus global mean bias and b) correlation versus global mean bias compared to GMD observations form March-May. Large circles represent the RefGMI (red), RefCOonly (black), and COonlySD (purple) simulations. Small circles show the impact of changing global or NH OH in the RefCOonly simulation.
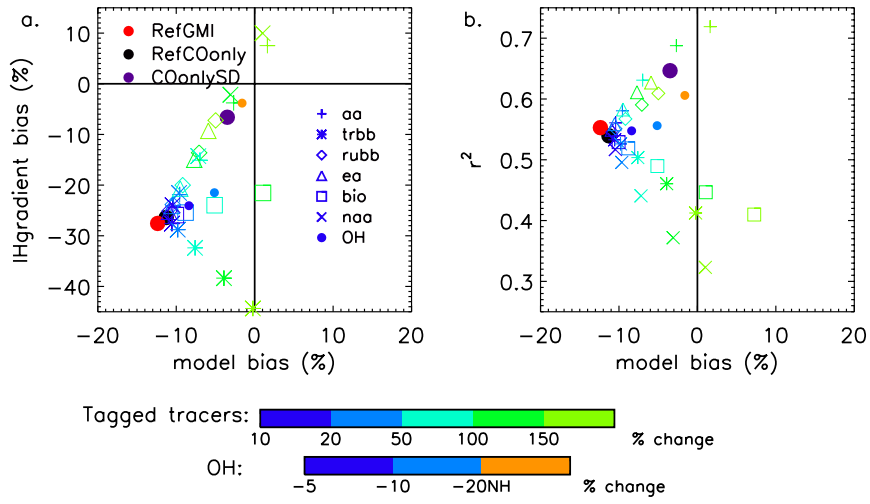
1

2

3 **Figure 5: As in Figure 4, but for June through August.**

4

49
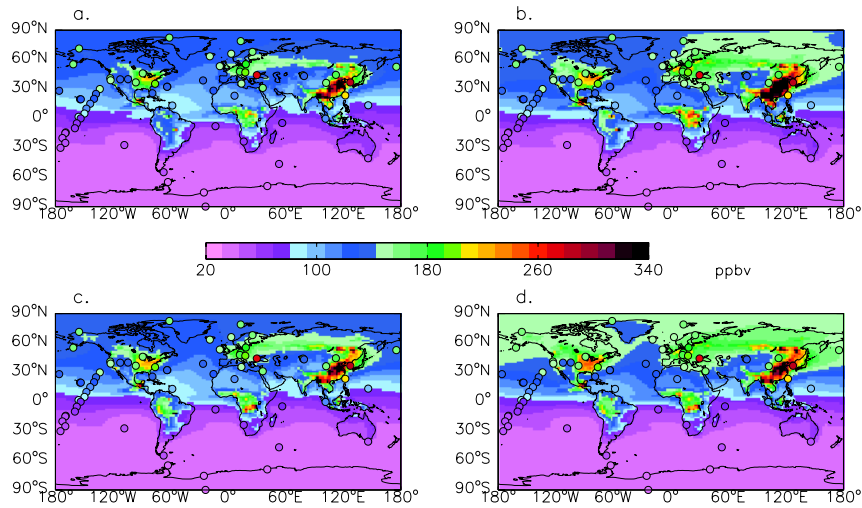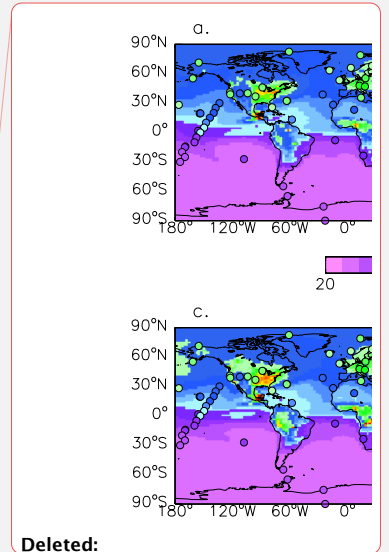
Figure 6: CO for March through May of 1999-2009 from the GMD observations (circles) overplotted on the surface CO from (a) RefGMI, (b) GMI-HiEmis, (c) RefCOonly, and (d) COonlyLowNHOH simulations.
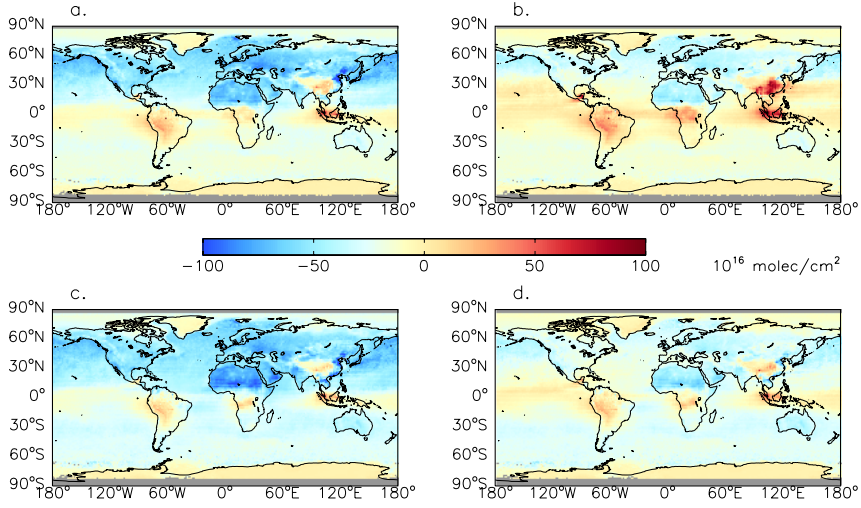
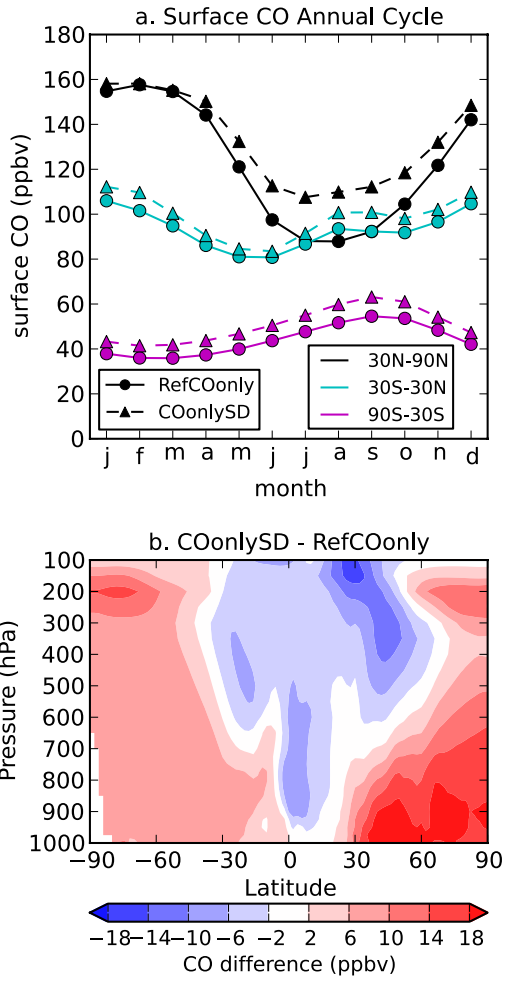**Figure 7: March through May difference between the simulated CO columns and MOPITT averaged over 2000-2009 for the (a) RefGMI, (b) GMI-HiEmis, (c) RefCOonly, and (d) COonlyLowNHOH simulations. The simulated CO is convolved with the MOPITT averaging kernels and a priori.**

Figure 8: (a) Annual cycle of surface CO in the RefCOonly simulation (circles) and COonlySD simulation (triangles) for 30°N-90°N (black), 30°S-30°N (cyan), and 90°S-30°S (magenta). (b) Annual zonal mean cross section of the difference in CO between the COonlySD and RefCOonly simulations.

1
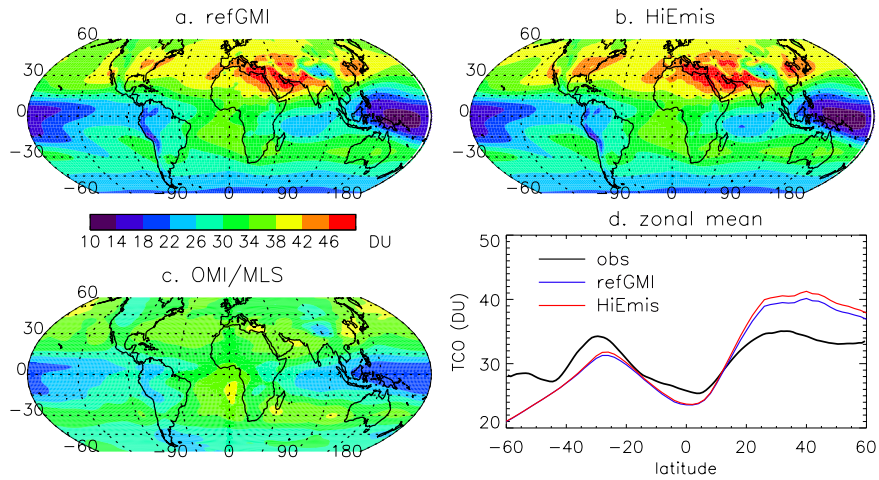
Figure 9: Annual mean tropospheric column ozone (TCO) from the RefGMI (a) and GMI-HiEmis (b) simulations compared to the OMI/MLS TCO product (c) of (Ziemke et al., 2011). Panel d compares the zonal mean simulated and OMI/MLS values. The simulated values are averaged over the years of the timeslice (1999-2009).
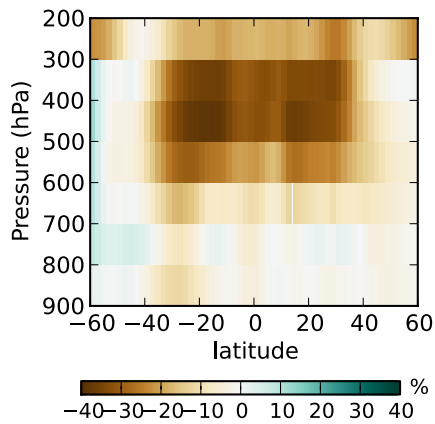
7

1　**Figure 10: Annual mean percent change in specific humidity imposed in the CO-**

2　**OHSensQ experiment between 900 and 200 hPa, 60°S-60°N.**
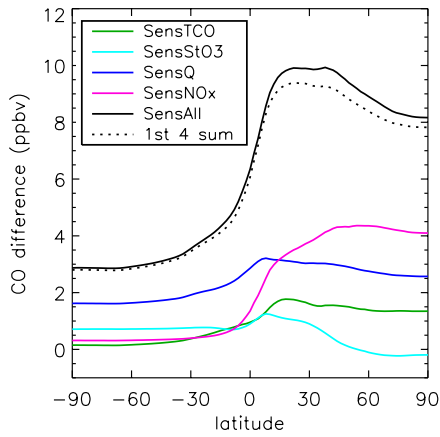
3

4　**Figure 11: Zonal mean surface CO difference compared to RefCO-OH for the CO-**

5　**OHSensTCO (green), CO-OHSensStO3 (cyan), CO-OHSensQ (blue), CO-**

6　**OHSensNOx (pink), and CO-OHSensAll (solid black) simulations averaged over**

7　**March through August of 2005 to 2009. The sum of the differences for the CO-**

8　**OHSensTCO, CO-OHSensStO3, CO-OHSensQ, and CO-OHSensNOx compared to**

9　**RefCO-OH is shown in the black dotted line.**

10